DETECTION OF AGNOPROTEIN EXPRESSION IN CLINICAL SAMPLES

Agnoprotein is expressed in JCV-infected oligodendrocytes and astrocytes in PML where it is located in the cytoplasm (Del Valle et al., 2002b). In the PML brain, immunoreactive signal for agnoprotein was distributed in the perinuclear areas and cytoplasmic processes with occasional punctate staining in demyelinating lesions as well as adjacent myelinated areas (Okada et al., 2002). Figure 3A shows immunohistochemical staining of PML brain tissue with antibody to JCV agnoprotein. JCV agnoprotein is present in the cytoplasm in a perinuclear fashion.

There is evidence that JCV is associated with some human cancers especially brain tumors (reviewed in White and Khalili, 2004a,b). It has recently been found that some of these JCV-associated tumors express agnoprotein. Immunohistochemical analysis of 20 well-characterized medulloblastomas showed expression of agnoprotein in the neoplastic cells in 11 of the samples (Del Valle et al., 2002b). A similar fraction of oligodendrogliomas samples exhibited immunoreactivity for expression of agnoprotein (Del Valle et al., 2002a). Agnoprotein expression has been detected in colon cancer (Enam et al., 2002), primary central nervous system lymphoma (Del Valle et al., 2004a), and esophageal cancer (Del Valle et al., 2004b). In tumor tissues, agnoprotein exhibits its characteristic perinuclear localization. Figure 3B shows immunohistochemical staining of medulloblastoma tissue with antibody to JCV agnoprotein.

RNA INTERFERENCE (RNAi) APPROACHES FOR THE STUDY OF JCV AGNOPROTEIN

RNAi is a conserved biological response to double-stranded RNA that mediates resistance to parasitic and pathogenic nucleic acids, and regulates gene expression (Hannon, 2002). This approach may revolutionize mammalian virology and may also yield new therapeutic approaches to viral infections (Jacque et al., 2002; Gitlin and Andino, 2003). Effective inhibition of JCV gene expression and replication is a critical target for the therapy of PML and RNAi aimed at viral proteins, including agnoprotein, represents a promising line of attack. Radhakrishnan et al. (2004) utilized small interfering RNAs (siRNAs) to target T-antigen and agnoprotein in JCV-infected primary human astrocytes. T-antigen siRNA caused a >50% decline in the level of T antigen and its transcriptional activity upon the viral capsid genes as well as reducing viral replication. Similarly agnoprotein siRNA drastically suppressed agnoprotein production. Interestingly, the agnoprotein siRNA also substantially reduced the expression of T-antigen and VP1 in the JCV-infected cells. When both T-antigen and agnoprotein siRNAs were used in combination, expression of T-antigen and VP1 were completely abolished (Radhakrishnan et al., 2004).

Orba et al. (2004) used the JCV/SVEΔ virus and SVG-A cell system (described above) to examine the effects of siRNAs that target late viral proteins including agnoprotein and VP1. These siRNAs caused a marked inhibition of both viral protein expression and of virus production. Agnoprotein siRNA inhibited both agnoprotein and VP1 expression and this was likely due to the degradation of the polycistronic late RNA that encodes both of these proteins (Orba et al., 2004).

The used agnoprotein siRNA is an important approach to furthering the understanding of the molecular biology of agnoprotein and demonstrates that it is a potential therapeutic target for the treatment of PML.

AGNOPROTEINS OF NON-PRIMATE POLYOMAVIRUSES

Besides the three primate polyomaviruses (SV40, JCV, and BKV), there are at least two other examples of polyomaviruses with a non-rodent genome arrangement, i.e., two, rather than three, forms of T antigen encoded in the early region. Bovine polyomavirus (BPV) has been recognized as a contaminant of certain batches of fetal calf serum where it can be detected by PCR or viral replication in bovine kidney cells (Nairn et al., 2003). The complete nucleotide sequence of BPV revealed the presence of an agnogene that is predicted to encode a 118 amino acid protein (Schuurman et al., 1990). The BPV agnogene is located in the leader region of the late region and its sequence predicts an agnoprotein that has detectable sequence homology to the primate agnoproteins: it has a 33% sequence identity with JCV agnoprotein over a 45 amino acid region. However, it is significantly larger and more acidic than JCV agnoprotein and no studies have been performed to investigate the function of the putative BPV agnoprotein. Budgerigar fledgling disease virus (BFDV, BFDV-1) is a polyomavirus and is the etiological agent of an acute fatal disease of young parakeets. The late

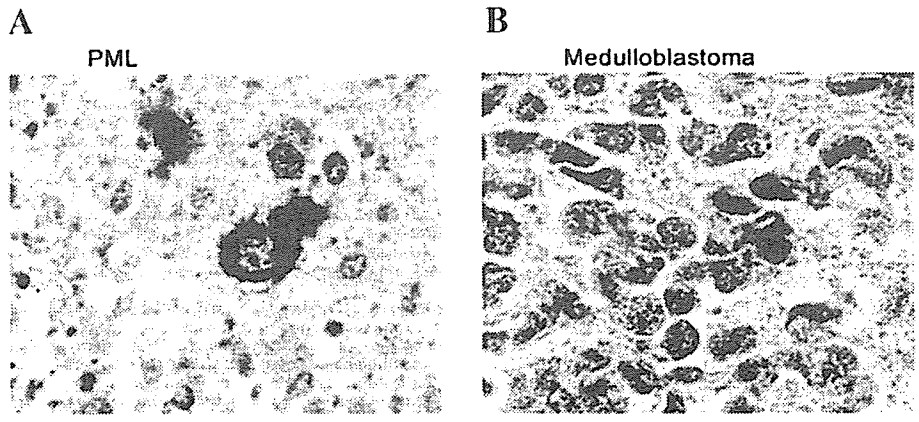

Fig. 3. Immunohistochemical analysis of JCV agnoprotein expression in progressive multifocal leukoencephalopathy (PML) and medulloblastoma. The JCV agnoprotein was detected with a polyclonal antibody developed in our laboratory. **A**: PML. **B**: Medulloblastoma.

mRNA 5′-ends define two putative promoters (p1 and p2) and as a result of incomplete and/or alternative splicing, the late polycistronic mRNAs contain two sets of two ORFs encoding four agnoproteins designated agno-1a, agno-1b, agno-2a, and agno-2b (Luo et al., 1995). Agno-1a is essential to the virus life cycle (Liu and Hobom, 2000) and is incorporated into the viral capsid as a fourth structural protein, VP4 (Johne and Muller, 2001). Agno-1b is essentially an internally deleted form of agno-1a (Liu et al., 2000). Agno-2a and agno-2b are splice variants that share a common N-terminus. Like the agnoprotein of primate polyomaviruses, these proteins are small and highly basic. Furthermore the agno-2 N-terminus shares significant sequence similarity with the N-terminus of JCV agnoprotein (32% sequence identity over 38 amino acids). Finally, when His-tagged Agno-2a and Agno-2b were expressed in MDCK cells, they were shown to have a perinuclear and cytoplasmic localization (Liu and Hobom, 1999). Thus, agnoprotein function may not be confined solely to the primate polyomaviruses.

EARLY LEADER PROTEINS (ELPs)

During SV40 lytic infection, a shift in the location of the start sites of the early mRNAs to an upstream position occurs with the onset of DNA replication. Within the additional leader sequence of the late-early transcripts is encoded an SV40 early leader protein (SELP) that can be detected by pulse labeling in vivo as a 2.7-kDa peptide that accumulates at late times after lytic infection (Khalili et al., 1987a). SELP is 23 amino acids in length and has a predicted isoelectric point of 9.8. A similar upstream shift in start site for early mRNA occurs during JCV and BKV infection (Khalili et al., 1987b; Frisque and White, 1992) and analogous peptides are predicted to exist for these viruses. The position of ELP in the polyomavirus genome is shown in Figure 1A. Putative JCV ELP (JELP) is 38 amino acids in length with a predicted size of 4.3-kDa and pI of 10.5, while that of BKV (BELP) is 39 amino acids in length with a predicted size of 4.4-kDa and a pI of 10.4. The ELPs are predicted to share a high degree of homology (Fig. 4): JELP has a predicted 70% amino acid sequence identity to BELP in a 30 amino acid overlap and 62% identity to SELP in a 21 amino acid overlap. This conservation of primary structure between ELPs suggests that they are functionally important and an investigation of their molecular biology might be a fruitful area of research. In the case of JCV, there exists a second potential ELP of 28 amino acids that lies within the JELP region but in a different reading frame.

```
                10          20          30
JELP  MSSCLAGSHPFPFFYI YRRPRPPPPPSLLRSSKGVEAF
                |  ||:| |:|||||  || :| ||||||||
BELP     MGKQLLPVAFFFIIYKRPRPPLPPPFLSSSKGVEAFSEA
                       :|||||  | |   ||:  ||| ||
SELP                   MQRPRPPRPLSYSRSSE  EAFLEA
                                  10          20
```

Fig. 4. Comparison of the predicted amino acid sequence of JCV early leader protein (JELP) to that of BKV (BELP) and SV40 (SELP). The predicted amino acid sequence of JELP was compared to the sequences of BELP and SELP (Khalili et al., 1987a). Sequence identity is indicated with a tilde (|). Conservative sequence changes are indicated with a colon (:). Amino acids that are identical in all three polyomaviruses are shown in bold face. Alignment was generated with the FASTA algorithm (Lipman and Pearson, 1985).

CONCLUSIONS

The early regulatory proteins of the primate polyomaviruses, large-T and small-t, have received considerable attention and much is now understood about their role in the viral life cycle and in cellular transformation. On the other hand, agnoprotein has received less attention. The literature contains only about 40 research papers on agnoprotein, and all are cited herein. However, it is becoming clear that agnoprotein has a role, not only in the replicative life-cycle of polyomaviruses, but also in the dysregulation of cellular processes such as cell cycle control and DNA repair that may contribute to neoplasia. Investigating agnoprotein function is important for understanding polyomaviral diseases such as PML and offers therapeutic possibilities as discussed above. The expression of agnoprotein in clinical samples of some human cancers provides another indication of its possible role in cellular transformation and another avenue for research. There is still much to be learned about agnoprotein and possible future directions include elucidating its cellular protein binding partners, its interactions with other viral proteins during virion assembly and its possible modulation by post-transcriptional modifications. Similar approaches could be adopted for the ELPs about which almost nothing is known.

ACKNOWLEDGMENTS

We thank Dr. Luis Del Valle for the immunohistochemistry. We thank past and present members of the Center for Neurovirology and Cancer Biology for their insightful discussion and sharing of ideas and reagents. We also thank C. Schriver for editorial assistance.

LITERATURE CITED

Aloni Y, Hay N. 1983. Attenuation and modulation of mRNA secondary structure in a feedback control system regulating SV40 gene expression. Mol Biol Rep 9:91–100.

Barkan A, Welch RC, Mertz JE. 1987. Missense mutations in the *VP1* gene of simian virus 40 that compensate for defects caused by deletions in the viral agnogene. J Virol 61:3190–3198.

Berger JR. 2003. Progressive multifocal leukoencephalopathy in acquired immuno-deficiency syndrome: Explaining the high incidence and disproportionate frequency of the illness relative to other immunosuppressive conditions. J Neurovirol 9(Suppl 1):38–41.

Bollag B, Prins C, Snyder EL, Frisque RJ. 2000. Purified JC virus T and T′ proteins differentially interact with the retinoblastoma family of tumor suppressor proteins. Virology 274:165–178.

Carswell S, Alwine JC. 1986. Simian virus 40 agnoprotein facilitates perinuclear-nuclear localization of VP1, the major capsid protein. J Virol 60:1055–1061.

Carswell S, Resnick J, Alwine JC. 1986. Construction and characterization of CV-1P cell lines which constitutively express the simian virus 40 agnoprotein: Alteration of plaquing phenotype of viral agnogene mutants. J Virol 60:415–422.

Cole CN. 1996. Polyomavirinae: The viruses and their replication. In: Fields BN, Knipe DM, Howley PM, editors. Fundamental virology, 3rd edn. Philadelphia: Lippincott, Williams & Wilkins. pp 917–946.

Cubitt CL, Cui X, Agostini HT, Nerurkar VR, Scheirich I, Yanagihara R, Ryschkewitsch CF, Stoner GL. 2001. Predicted amino acid sequences for 100 JCV strains. J Neurovirol 7:339–344.

Dabrowski C, Alwine JC. 1988. Translational control of synthesis of simian virus 40 late proteins from polycistronic 19S late mRNA. J Virol 62:3182–3192.

Darbinyan A, Darbinian N, Safak M, Radhakrishnan S, Giordano A, Khalili K. 2002. Evidence for dysregulation of cell cycle by human polyomavirus, JCV, late auxiliary protein. Oncogene 21:5574–5581.

Darbinyan A, Siddiqui KM, Slonina D, Darbinian N, Amini S, White MK, Khalili K. 2004. Role of JCV agnoprotein in DNA repair. J Virol 78:8593–8600.

Del Valle L, Enam S, Lara C, Ortiz-Hidalgo C, Katsetos CD, Khalili K. 2002a. Detection of JC polyomavirus DNA sequences and cellular localization of T-antigen and agnoprotein in oligodendrogliomas. Clin Cancer Res 8:3332–3340.

Del Valle L, Gordon J, Enam S, Delbue S, Croul S, Abraham S, Radhakrishnan S, Assimakopoulou M, Katsetos CD, Khalili K. 2002b. Expression of human neurotropic polyomavirus JCV late gene product agnoprotein in human medulloblastoma. J Natl Cancer Inst 94:267–273.

Del Valle L, Enam S, Lara C, Miklossy J, Khalili K, Gordon J. 2004a. Primary central nervous system lymphoma expressing the human neurotropic polyomavirus, JC virus genome. J Virol 78:3462–3469.

Del Valle L, White MK, Enam S, Piña-Oviedo S, Bromer MQ, Thomas RM, Parkman HP, Khalili K. 2004b. Detection of JC virus DNA sequences and expression of viral T-antigen and agnoprotein in esophageal cancer. Cancer (in press).

Dhar R, Subramanian KN, Pan J, Weissman SM. 1977. Structure of a large segment of the genome of simian virus 40 that does not encode known proteins. Proc Natl Acad Sci USA 74:827–831.
Enam S, Del Valle L, Lara C, Gan DD, Ortiz-Hidalgo C, Palazzo JP, Khalili K. 2002. Association of human polyomavirus JCV with colon cancer: Evidence for interaction of viral T-antigen and beta-catenin. Cancer Res 62:7093–7101.
Endo S, Okada Y, Orba Y, Nishihara H, Tanaka S, Nagashima K, Sawa H. 2003. JC virus agnoprotein colocalizes with tubulin. J Neurovirol 9(Suppl 1):10–14.
Fiers W, Contreras R, Haegemann G, Rogiers R, Van de Voorde A, Van Heuverswyn H, Van Herreweghe J, Volckaert G, Ysebaert M. 1978. Complete nucleotide sequence of SV40 DNA. Nature 273:113–120.
Frisque RJ. 2001. Structure and function of JC virus T′ proteins. J Neurovirol 7:293–297.
Frisque RJ, White FA. 1992. The molecular biology of JC virus, causative agent of progressive multifocal leukoencephalopathy. In: Roos RP, editor. Molecular neurovirology. Totowa, NJ: Humana Press. pp 25–158.
Frisque RJ, Bollag B, Tyagarajan SK, Kilpatrick LH. 2003. T′ proteins influence JC virus biology. J Neurovirol 9(Suppl 1):15–20.
Garnier J, Osguthorpe DJ, Robson B. 1978. Analysis of the accuracy and implications of simple methods for predicting the secondary structure of globular proteins. J Mol Biol 120:97–120.
Gitlin L, Andino R. 2003. Nucleic acid-based immune system: The antiviral potential of mammalian RNA silencing. J Virol 77:7159–7165.
Grass DS, Manley JL. 1987. Selective translation initiation on bicistronic simian virus 40 late mRNA. J Virol 61:2331–2335.
Hannon GJ. 2002. RNA interference. Nature 418:244–251.
Hay N, Aloni Y. 1985. Attenuation of late simian virus 40 mRNA synthesis is enhanced by the agnoprotein and is temporally regulated in isolated nuclear systems. Mol Cell Biol 5:1327–1334.
Hay N, Kessler M, Aloni Y. 1984. SV40 deletion mutant (d1861) with agnoprotein shortened by four amino acids. Virology 137:160–170.
Hou-Jong MH, Larsen SH, Roman A. 1987. Role of the agnoprotein in regulation of simian virus 40 replication and maturation pathways. J Virol 61:937–939.
Jackson V, Chalkley R. 1981. Use of whole-cell fixation to visualize replicating and maturing simian virus 40: Identification of new viral gene product. Proc Natl Acad Sci USA 78:6081–6085.
Jacque JM, Triques K, Stevenson M. 2002. Modulation of HIV-1 replication by RNA interference. Nature 418:435–438.
Jay G, Nomura S, Anderson CW, Khoury G. 1981. Identification of the SV40 agnogene product: A DNA binding protein. Nature 291:346–349.
Jobes DV, Friedlaender JS, Mgone CS, Koki G, Alpers MP, Ryschkewitsch CF, Stoner GL. 1999. A novel JC virus variant found in the Highlands of Papua New Guinea has a 21-base pair deletion in the agnoprotein gene. J Hum Virol 2:350–358.
Johne R, Muller H. 2001. Avian polyomavirus agnoprotein 1a is incorporated into the virus particle as a fourth structural protein, VP4. J Gen Virol 82:909–918.
Khalili K, Brady J, Khoury G. 1987a. Translational regulation of SV40 early mRNA defines a new viral protein. Cell 48:639–645.
Khalili K, Feigenbaum L, Khoury G. 1987b. Evidence for a shift in 5′-termini of early viral RNA during the lytic cycle of JC virus. Virology 158:469–472.
Khalili K, Brady J, Pipas JM, Spence SL, Sadofsky M, Khoury G. 1988. Carboxyl-terminal mutants of the large tumor antigen of simian virus 40: A role for the early protein late in the lytic cycle. Proc Natl Acad Sci USA 85:354–358.
Krynska B, Del Valle L, Croul S, Gordon J, Katsetos CD, Carbone M, Giordano A, Khalili K. 1999. Detection of human neurotropic JC virus DNA sequence and expression of the viral oncogenic protein in pediatric medulloblastomas. Proc Natl Acad Sci USA 96:11519–11524.
Lipman DJ, Pearson WR. 1985. Rapid and sensitive protein similarity searches. Science 227:1435–1441.
Liu Q, Hobom G. 1999. Recombinant expression of late genes agno-2a and agno-2b of avian polyomavirus BFDV. Virus Genes 19:183–187.
Liu Q, Hobom G. 2000. Agnoprotein-1a of avian polyomavirus budgerigar fledgling disease virus: Identification of phosphorylation sites and functional importance in the virus life-cycle. J Gen Virol 81:359–367.
Liu Q, Hintz M, Li J, Linder M, Geyer R, Hobom G. 2000. Recombinant expression and modification analysis of protein agno-1b encoded by avian polyomavirus BFDV. Arch Virol 145:1211–1223.
Luo D, Muller H, Tang XB, Hobom G. 1995. Early and late pre-mRNA processing of budgerigar fledgling disease virus 1: Identification of viral RNA 5′ and 3′ ends and internal splice junctions. J Gen Virol 76:161–166.
Margolskee RF, Nathans D. 1983. Suppression of a VP1 mutant of simian virus 40 by missense mutations in serine codons of the viral agnogene. J Virol 48: 405–409.
Mertz JE, Murphy A, Barkan A. 1983. Mutants deleted in the agnogene of simian virus 40 define a new complementation group. J Virol 45:36–46.
Nairn C, Lovatt A, Galbraith DN. 2003. Detection of infectious bovine polyomavirus. Biologicals 31:303–306.
Ng SC, Mertz JE, Sanden-Will S, Bina M. 1985. Simian virus 40 maturation in cells harboring mutants deleted in the agnogene. J Biol Chem 260:1127–1132.
Nomura S, Khoury G, Jay G. 1983. Subcellular localization of the simian virus 40 agnoprotein. J Virol 45:428–433.
Nomura S, Jay G, Khoury G. 1986. Spontaneous deletion mutants resulting from a frameshift insertion in the simian virus 40 agnogene. J Virol 58:165–172.
Okada Y, Endo S, Takahashi H, Sawa H, Umemura T, Nagashima K. 2001. Distribution and function of JCV agnoprotein. J Neurovirol 7:302–306.
Okada Y, Sawa H, Endo S, Orba Y, Umemura T, Nishihara H, Stan AC, Tanaka S, Takahashi H, Nagashima K. 2002. Expression of JC virus agnoprotein in progressive multifocal leukoencephalopathy brain. Acta Neuropathol (Berl) 104:130–136.
Orba Y, Sawa H, Iwata H, Tanaka S, Nagashima K. 2004. Inhibition of virus production in JC virus-infected cells by postinfection RNA interference. J Virol 78:7270–7273.
Perez L, Wills JW, Hunter E. 1987. Expression of the Rous sarcoma virus *env* gene from a simian virus 40 late-region replacement vector: Effects of upstream initiation codons. J Virol 61:1276–1281.
Prins C, Frisque RJ. 2001. JC virus T′ proteins encoded by alternatively spliced early mRNAs enhance T antigen-mediated viral DNA replication in human cells. J Neurovirol 7:250–264.
Radhakrishnan S, Otte J, Enam S, Del Valle L, Khalili K, Gordon J. 2003. JC virus-induced changes in cellular gene expression in primary human astrocytes. J Virol 77:10638–10644.
Radhakrishnan S, Gordon J, Del Valle L, Cui J, Khalili K. 2004. Intracellular approach for blocking JC virus gene expression by using RNA interference during viral infection. J Virol 78:7264–7269.
Reddy VB, Thimmappaya B, Dhar R, Subramanian KN, Zain BS, Pan J, Ghosh PK, Celma ML, Weissman SM. 1978. The genome of simian virus 40. Science 200:494–502.
Resnick J, Shenk T. 1986. Simian virus 40 agnoprotein facilitates normal nuclear location of the major capsid polypeptide and cell-to-cell spread of virus. J Virol 60:1098–1106.
Rinaldo CH, Traavik T, Hey A. 1998. The agnogene of the human polyomavirus BK is expressed. J Virol 72:6233–6236.
Safak M, Barrucco R, Darbinyan A, Okada Y, Nagashima K, Khalili K. 2001. Interaction of JC virus agno protein with T antigen modulates transcription and replication of the viral genome in glial cells. J Virol 75:1476–1486.
Safak M, Sadowska B, Barrucco R, Khalili K. 2002. Functional interaction between JC virus late regulatory agnoprotein and cellular Y-box binding transcription factor, YB-1. J Virol 76:3828–3838.
Schuurman R, Sol C, van der Noordaa J. 1990. The complete nucleotide sequence of bovine polyomavirus. J Gen Virol 71:1723–1735.
Sedman SA, Gelembiuk GW, Mertz JE. 1990. Translation initiation at a downstream AUG occurs with increased efficiency when the upstream AUG is located very close to the 5′ cap. J Virol 64:453–457.
Spence SL, Pipas JM. 1994. Simian virus 40 large T antigen host range domain functions in virion assembly. J Virol 68:4227–4240.
Spence SL, Tack LC, Wright JH, Carswell S, Pipas JM. 1990. Infection of CV1 cells expressing the polyoma virus middle T antigen or the SV40 agnogene product with simian virus 40 host-range mutants. In Vitro Cell Dev Biol 26: 604–611.
Stacy T, Chamberlain M, Cole CN. 1989. Simian virus 40 host range/helper function mutations cause multiple defects in viral late gene expression. J Virol 63:5208–5215.
Stacy TP, Chamberlain M, Carswell S, Cole CN. 1990. The growth of simian virus 40 (SV40) host range/adenovirus helper function mutants in an African green monkey cell line that constitutively expresses the SV40 agnoprotein. J Virol 64:3522–3526.
Trowbridge PW, Frisque RJ. 1995. Identification of three new JC virus proteins generated by alternative splicing of the early viral mRNA. J Neurovirol 1:195–206.
von Heijne G. 1981. On the hydrophobic nature of signal sequences. Eur J Biochem 116:419–422.
White MK, Khalili K. 2004a. Polyomaviruses and human cancer: Molecular mechanisms underlying patterns of tumorigenesis (Mini-Review). Virology 324:1–16.
White MK, Khalili K. 2004b. Signaling pathways and polyomavirus oncoproteins: Importance in malignant transformation. Gene Ther Mol Biol 8:19–30.

EMBO
reports

scientific report

Dissociation of heterochromatin protein 1 from lamin B receptor induced by human polyomavirus agnoprotein: role in nuclear egress of viral particles

Yuki Okada[1,2,3], Tadaki Suzuki[1,3*], Yuji Sunden[1,2,3], Yasuko Orba[1,3], Shingo Kose[5], Naoko Imamoto[5], Hidehiro Takahashi[6], Shinya Tanaka[1,3], William W. Hall[7], Kazuo Nagashima[1,3] & Hirofumi Sawa[3,4,8+]*

[1]Laboratory of Molecular and Cellular Pathology, and [2]Laboratory of Comparative Pathology, Graduate School of Hokkaido University, Sapporo, Japan, [3]CREST, JST, Sapporo, Japan, [4]21st Century COE Program for Zoonosis Control, Graduate School of Hokkaido University, Sapporo, Japan, [5]Cellular Dynamics Laboratory, RIKEN, Discovery Research Institute, Wako, Saitama, Japan, [6]Department of Pathology, NIHD, Toyama, Shinjuku, Tokyo, Japan, [7]Department of Medical Microbiology, University College, Dublin, Ireland, and [8]Department of Molecular Biology and Diagnosis, Hokkaido University Research Center for Zoonosis Control, Sapporo, Japan

The nuclear envelope is one of the chief obstacles to the translocation of macromolecules that are larger than the diameter of nuclear pores. Heterochromatin protein 1 (HP1) bound to the lamin B receptor (LBR) is thought to contribute to reassembly of the nuclear envelope after cell division. Human polyomavirus agnoprotein (Agno) has been shown to bind to HP1α and to induce its dissociation from LBR, resulting in destabilization of the nuclear envelope. Fluorescence recovery after photobleaching showed that Agno increased the lateral mobility of LBR in the inner nuclear membrane. Biochemical and immunofluorescence analyses showed that Agno is targeted to the nuclear envelope and facilitates the nuclear egress of polyomavirus-like particles. These results indicate that dissociation of HP1α from LBR and consequent perturbation of the nuclear envelope induced by polyomavirus Agno promote the translocation of virions out of the nucleus.

[1]Laboratory of Molecular and Cellular Pathology, and [2]Laboratory of Comparative Pathology, Graduate School of Hokkaido University, N15, W7, Kita-ku, Sapporo 060-8638, Japan
[3]CREST, JST, Sapporo 060-8638, Japan
[4]21st Century COE Program for Zoonosis Control, Graduate School of Hokkaido University, Sapporo 060-8638, Japan
[5]Cellular Dynamics Laboratory, RIKEN, Discovery Research Institute, Wako, Saitama 351-0198, Japan
[6]Department of Pathology, NIHD, Toyama, Shinjuku, Tokyo 162-8640, Japan
[7]Department of Medical Microbiology, University College, Dublin 4, Ireland
[8]Department of Molecular Biology and Diagnosis, Hokkaido University Research Center for Zoonosis Control, Sapporo 060-8638, Japan
*These authors contributed equally to this work
+Corresponding author. Tel/Fax: +81 11 706 7806;
E-mail: h-sawa@patho2.med.hokudai.ac.jp

Received 6 September 2004; revised 21 March 2005; accepted 24 March 2005; published online 29 April 2005

Keywords: agnoprotein; heterochromatin protein 1; JC virus; lamin B receptor
EMBO reports (2005) 6, 452–457. doi:10.1038/sj.embor.7400406

INTRODUCTION

The nuclear envelope (NE) consists of an outer nuclear membrane, an inner nuclear membrane (INM), nuclear pore complexes and the peripheral nuclear lamina located adjacent to the INM. Various proteins of chromatin (histones, heterochromatin protein 1 (HP1), barrier-to-autointegration factor), the nuclear lamina (lamins A, B and C) and the INM (emerin, lamina-associated polypeptide 2β, lamin B receptor (LBR); Salina *et al*, 2001) associate with each other during reconstitution and stabilization of the NE. LBR is an integral protein of the INM and binds to HP1 proteins (Ye & Worman, 1996; Ye *et al*, 1997). The NE presents one of the chief obstacles to transport from the nucleus to the cytoplasm of macromolecules, including the virions of most DNA viruses (Pante & Kann, 2002). The β-herpesvirus gene products UL31 and UL34 induce depolymerization of the nuclear lamina to facilitate the nuclear egress of viral capsids (Muranyi *et al*, 2002). However, the mechanisms by which other DNA viruses exit the nucleus remain unclear, including the JC virus (JCV), which is the causative agent of progressive multifocal leukoencephalopathy and belongs to the family of polyomaviruses. The JCV agnoprotein (Agno) comprises 71 amino acids, is localized predominantly in the perinuclear region and the cytoplasm of infected cells (Okada *et al*, 2002) and is related to DNA-damage-induced cell-cycle regulation (Darbinyan *et al*, 2004). The amino-acid sequence of JCV Agno shares ~60% homology with those of agnoproteins of other polyomaviruses; however, the sequence of the amino-terminal portion is ~90%

identical to those of other polyomaviruses, which is suggestive of conservation of function. We show that the N-terminal region of JCV Agno associates with HP1 *in vivo*, resulting in dissociation of HP1 from LBR. This effect alters the NE and thereby facilitates the release of progeny virions from the nucleus into the cytoplasm without nuclear disintegration.

RESULTS

Human JCV Agno binds to HP1

We initially performed a yeast two-hybrid screen with the conserved N-terminal 24 amino acids of JCV Agno as the bait. From a complementary DNA library of human embryonic kidney (HEK) 293 cells, which are permissive for JCV infection (Suzuki *et al*, 2001), six positive clones were isolated and were found to encode the entire sequence of HP1α and the chromo-shadow domain (CSD) of HP1γ (Fig 1A). Interaction between Agno and either Myc-epitope-tagged human HP1α (Fig 1B) or endogenous HP1α (Fig 1C) was also shown in HEK293 cells. We also performed an immunoprecipitation assay to examine whether Agno binds to HP1β and HP1γ *in vivo*, and found that Agno did not interact with HP1β and HP1γ (Fig 1D), although the CSD of HP1γ was identified by a yeast two-hybrid screening.

Agno interacts with HP1α at the NE

We have reported that the Agno is mainly expressed in the cytoplasm of infected cells (Okada *et al*, 2001), whereas HP1α is expressed in the nucleus. To examine where Agno and HP1α become associated, a mutant of Agno lacking most of the N-terminal HP1α-binding motif, designated C18, was constructed. Subcellular localizations of wild-type (WT) and a C18 mutant of Agno were predominantly observed in the cytoplasm (Fig 2A). Immunoprecipitation analysis showed that C18 did not interact with HP1α, whereas WT Agno bound to HP1α (Fig 2B). The C18 showed cytoplasmic distribution that was similar to WT; however, the C18 did not colocalize with lamin A/C at the NE (Fig 2C). These results indicated that the interaction between Agno and HP1α occurs at the NE.

Agno disrupts the interaction between HP1α and LBR

Some HP1 proteins may be partially localized in the perinuclear region and this may be because of LBR binding (Minc *et al*, 1999). Our yeast two-hybrid analysis indicated that Agno interacts with the CSD of HP1, which is also responsible for the association of these proteins with LBR (Ye *et al*, 1997). These observations led us

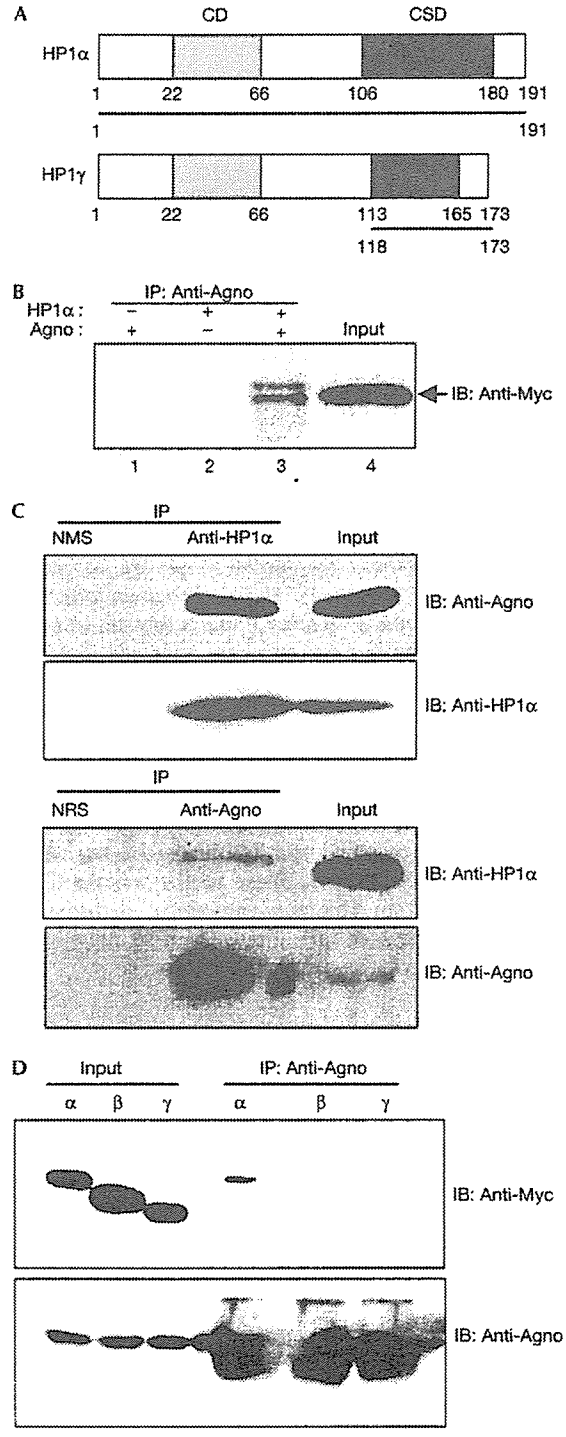

Fig 1 | Interaction of JCV Agno with HP1 *in vivo*. (A) Schematic representation of human HP1α and HP1γ showing the regions (bars) encoded by cDNA fragments isolated by a yeast two-hybrid assay with the N-terminal region of Agno as a bait. CD and CSD, chromo and chromo-shadow domains, respectively. (B) 293AG cells (HEK293 cells in which the expression of JCV Agno is inducible by Dox) were transfected with a vector for Myc-tagged human HP1α and were incubated in the absence or presence of Dox for 24 h. Cell lysates were subjected to immunoprecipitation with antibodies to Agno (anti-Agno), and the resulting precipitates were subjected to immunoblotting (IB) with anti-Myc. (C) Lysates prepared from 293AG cells after treatment with Dox for 48 h were subjected to immunoprecipitation with anti-HP1α or anti-Agno, and the resulting precipitates and cell lysates (Input) were subjected to immunoblotting with the same antibodies, as indicated. NMS, normal mouse serum; NRS, normal rabbit serum. (D) 293T cells were transfected with a vector for Agno and Myc-tagged human HP1α, β or γ, and were subjected to immunoprecipitation with anti-Agno. The resulting precipitates were subjected to immunoblotting with anti-Myc and anti-Agno.

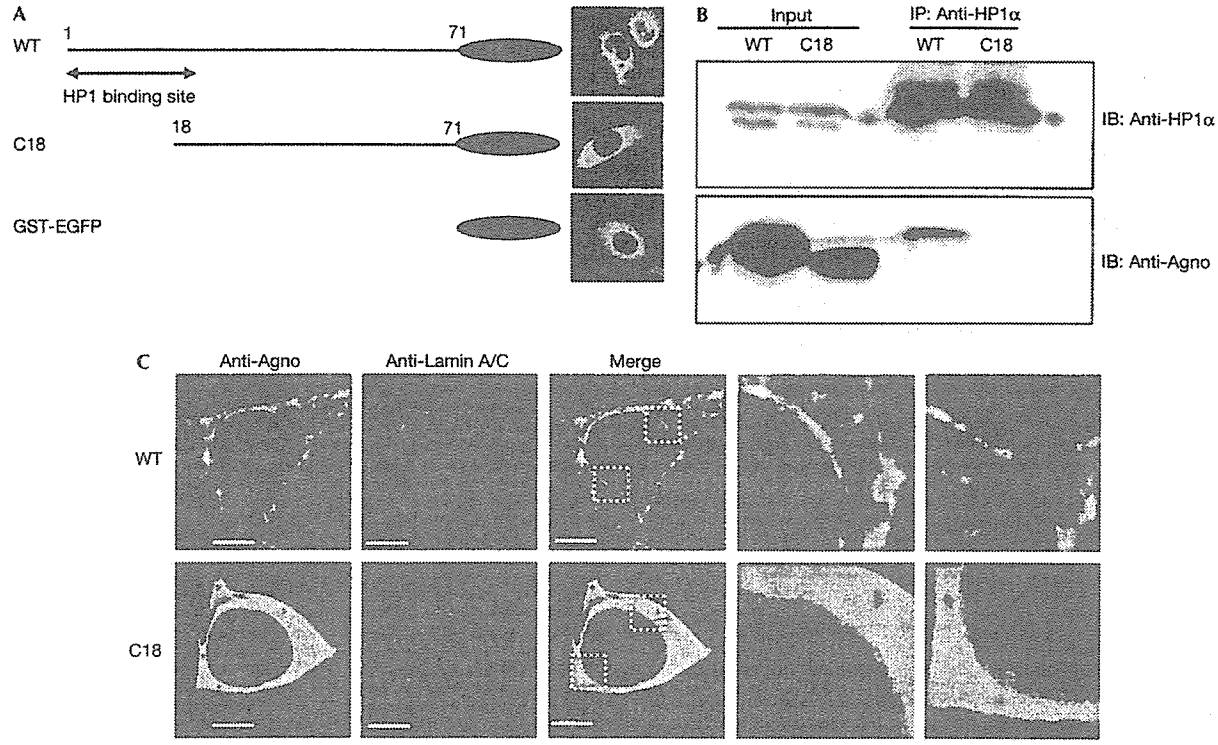

Fig 2 | Impaired ability of an Agno mutant to colocalize or interact with HP1. (A) Schematic representation of GST–EGFP fusion constructs of wild-type (WT) and mutant (C18) forms of Agno and EGFP fluorescence images showing their subcellular localizations in transfected HEK293 cells. (B) Lysates of 293T cells transiently expressing the WT or C18 forms of Agno were subjected to immunoprecipitation (IP) with anti-HP1α, and the resulting precipitates were subjected to immunoblotting (IB) with anti-Agno or anti-HP1α. (C) Immunofluorescence analysis of the expression of GST–EGFP-fused WT or C18 forms of Agno and of endogenous Lamin A/C in HEK293 cells. Enlarged dotted rectangles of the merged images are represented. Scale bars, 5 μm.

to propose that Agno might interfere with the interaction between HP1 and LBR and thereby alter the structure of the NE.

To examine this possibility, we established a cell line, designated 293AG, that is derived from HEK293 cells and in which the expression of JCV Agno subcloned into pcDNA4/TO/Myc–His is under the control of a tetracycline-responsive promoter. All 293AG cells expressed the recombinant Agno (~14 kDa) in 3 h of exposure to doxycycline (Dox), and the level of expression increased gradually with time (Fig 3A). In the absence of Dox, Agno was not detected by immunoblot or immunofluorescence analysis.

We next transfected 293AG cells with a vector for Myc-epitope-tagged HP1α (pCMV–MycHP1α) and subjected lysates prepared from Dox-treated or untreated cells to immunoprecipitation with antibodies to Agno. Immunoblot analysis with antibodies to Myc of precipitates prepared from the Dox-treated cells, but not of those from the untreated cells, showed the presence of HP1α (Fig 3B). We then transfected 293AG cells with both pCMV–MycHP1α and pLBR–EGFP (enhanced green fluorescent protein), and induced Agno expression with Dox treatment. The amount of HP1α that co-precipitated with Agno in these cells was directly related to the level of Agno expression (Fig 3B). Conversely, the amount of HP1α that co-precipitated with LBR–EGFP was inversely related to the level of Agno expression.

Agno increases the lateral mobility of LBR in the NE

Immunofluorescence analysis also showed that Agno colocalized with LBR–EGFP at the NE, and this colocalization was pronounced in invaginated regions of the NE (Fig 4A). The dissociation of LBR from heterochromatin results in structural changes in the NE, including the formation of invaginations and protrusions (Mazlo *et al*, 2001); such changes are also characteristic of JCV-infected oligodendrocytes in the brains of patients with progressive multifocal leukoencephalopathy.

Disruption of the interaction between HP1 and LBR by Agno might be expected to increase the lateral mobility of LBR in the NE. We examined this possibility by fluorescence recovery after photobleaching (FRAP) analysis in 293AG cells stably expressing LBR–EGFP. Photobleaching was induced at the nuclear rim, and recovery of fluorescence was monitored with a series of low-intensity scans. LBR–EGFP fluorescence in the bleached region of the nuclear rim recovered faster in cells expressing Agno than in those not exposed to Dox (Fig 4B,C); the mean recovery ratio at 10 min after photobleaching was significantly higher in the presence of Agno (Fig 4D). We also subjected the EGFP-fused full-length LBR (Haraguchi *et al*, 2000) to the FRAP analyses, and obtained results similar to those using the LBR–EGFP (data not shown). These observations indicated that Agno-induced dissociation of the LBR–HP1 complex resulted in an increase in the lateral mobility of LBR in the INM.

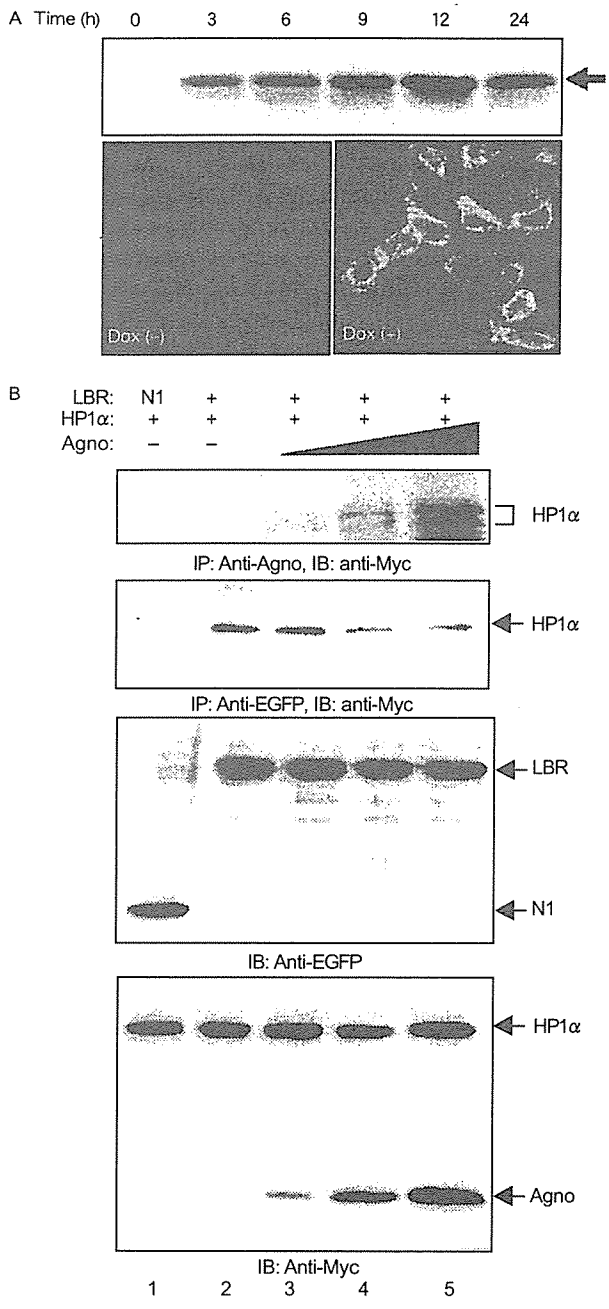

Fig 3 | Agno-induced dissociation of the HP1α–LBR complex *in vivo*. (A) 293AG cells were incubated with Dox for the indicated times, after which cell lysates were subjected to immunoblotting with anti-Agno. Cells incubated with or without Dox for 24 h were also subjected to immunofluorescence analysis with anti-Agno. (B) 293AG cells were transfected with pEGFP-N1 or pLBR–EGFP together with pCMV–MycHP1α. The transfected cells were treated with Dox for 0, 3, 7 or 24 h. Cell lysates were then subjected to immunoprecipitation (IP) with anti-Agno or anti-EGFP, and the resulting precipitates were subjected to immunoblotting (IB) with anti-Myc. Cell lysates were also subjected directly to immunoblotting with anti-EGFP or anti-Myc.

Agno facilitates nuclear egress of progeny virions

We proposed that the alteration of the NE induced by Agno might facilitate the nuclear release of progeny virions. To examine this possibility, we microinjected virus-like particles (VLPs) consisting of recombinant JCV VP1 into the nuclei of 293AG cells with or without Dox treatment. Such VLPs manifest a virion-like structure and physiological functions, including cellular attachment, intracytoplasmic transport and nuclear entry (Goldmann *et al*, 1999; Suzuki *et al*, 2001; Komagome *et al*, 2002; Qu *et al*, 2004), similar to those of JCV virions. We used Cy3 as a nuclear injection marker, which usually remained at the injection site. In the absence of Agno expression, most of the VLPs injected into the nucleus remained there 1 h later (Fig 5). In contrast, VLP fluorescence was not detected at this time in the nucleus of cells expressing Agno, suggesting that Agno promoted translocation of VLPs from the nucleus to the cytoplasm. Simultaneously, a certain amount of Cy3 also leaked into the cytoplasm in Dox (+) cells; however, it remained in the nucleus without Dox treatment. These observations indicate that the alteration of NE by Agno might facilitate nuclear egress of the progeny virions, and considering the behaviour of Cy3, this effect was not specific to virus particles.

DISCUSSION

The INM is linked to lamina and chromatin through interactions of its integral membrane proteins, including LBR. In the late stage of JCV infection, the nuclei of infected cells are filled with progeny virions and show structural alterations of the NE, such as invaginations and protrusions (Mazlo *et al*, 2001). We have shown that JCV Agno competes with LBR for binding to HP1, resulting in destabilization of the NE. Although viral protein-induced destabilization of the NE and a role for LBR have previously been described in herpesvirus infection (Scott & O'Hare, 2001; Muranyi *et al*, 2002), the role of LBR in this instance might be an indirect consequence of the depolymerization of lamin A/C that results from the virus-induced recruitment of protein kinase C to the INM. The association between LBR and its main ligand lamin B is also preserved during herpesvirus infection. LBR binds to a range of proteins (Ye & Worman, 1994, 1996), of which chromatin and chromatin-related proteins are thought to function as nucleoplasmic ligands that immobilize LBR in the INM (Ellenberg *et al*, 1997). LBR thus has a key role in the association of HP1 with the NE. Our data show that JCV Agno induces dissociation of HP1 from LBR by competitive binding to HP1, which caused an increase in the lateral mobility of LBR. This is the first evidence, to our knowledge, of a viral-protein-induced alteration of the NE through dissociation of HP1 and LBR.

In addition, expression of Agno also facilitated the nuclear export of VLPs without inducing nucleolysis, which is thought to mimic the nuclear egress of progeny virions in virus-infected cells. Consistent with this notion, agnogene-deficient simian virus 40 (SV40) shows a reduced capacity for cell-to-cell spread (Resnick & Shenk, 1986). Furthermore, we recently showed by RNA interference that JCV Agno is required for viral propagation (Orba *et al*, 2004). Together, our observations suggest that Agno facilitates viral propagation by promoting viral spreading. This function of JCV Agno is probably shared by agnoproteins of SV40 and human polyomavirus BK (BKV), given that the N-terminal region of JCV Agno is highly homologous to those of the SV40 and BKV proteins and is responsible for binding to HP1α.

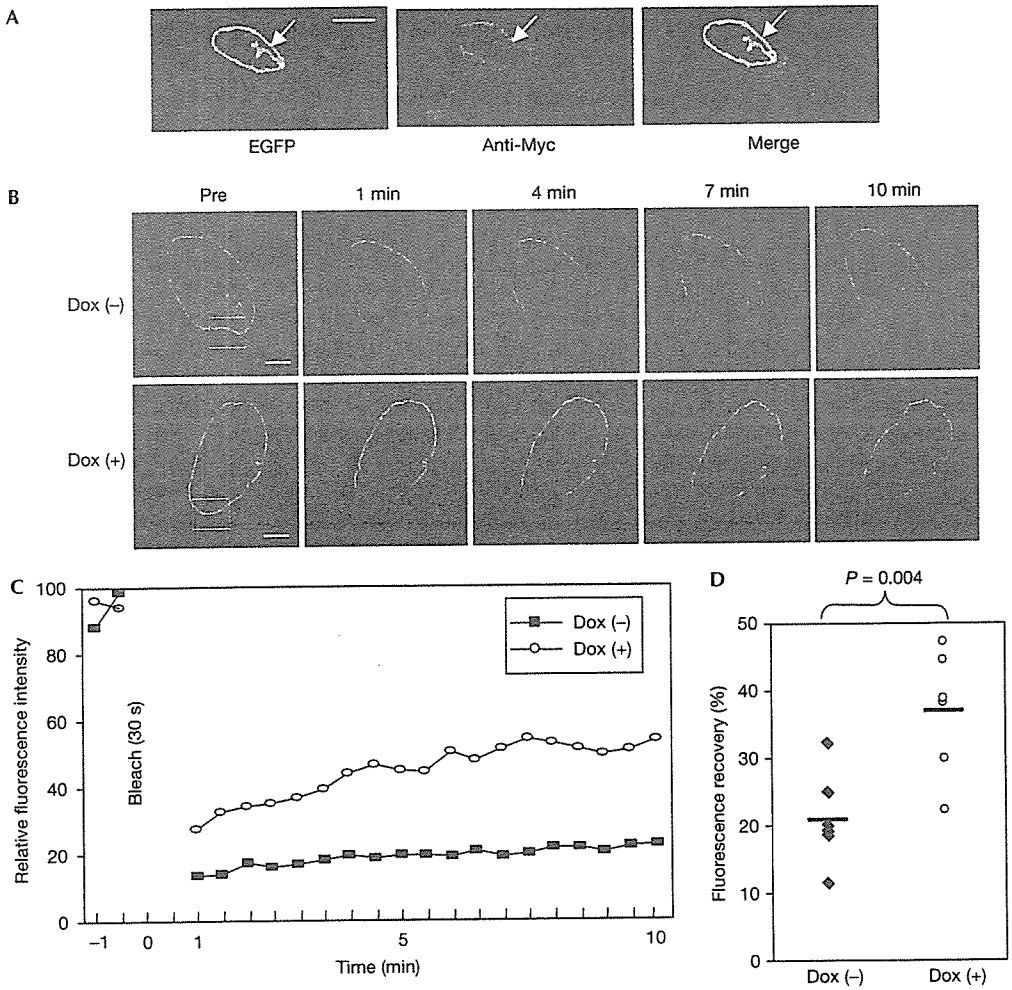

Fig 4 | Agno-induced increase in the lateral mobility of LBR. (A) Colocalization of LBR–EGFP detected by EGFP fluorescence and Agno detected with anti-Myc in 293AG cells. Arrows indicate an invagination of the NE in which LBR–EGFP and Agno are colocalized. Scale bar, 10 μm. (B) FRAP analysis of 293AG cells expressing LBR–EGFP and incubated in the absence or presence of Dox for 24 h. The fluorescence of LBR–EGFP in the boxed regions of the nuclear rim was irreversibly photobleached, and the recovery of fluorescence in these regions was monitored for 10 min. Representative images before (Pre) and at 1, 4, 7 and 10 min after bleaching are shown. Scale bars, 2 μm. (C) Quantification of the fluorescence recovery shown in (B). (D) Summary of fluorescence recovery ratios at 10 min after photobleaching. Each point represents an individual cell and the horizontal bars indicate the median values. The statistical significance of the difference between the two mean values was calculated by Student's two-tailed *t*-test.

METHODS

Plasmid construction. A cDNA encoding the first 238 amino acids of LBR was amplified by PCR from an HEK293 cell cDNA library and subcloned into pEGFP-N1 (BD Biosciences Clontech, Franklin Lakes, NJ, USA), yielding pLBR–EGFP (Gerlich *et al*, 2001; Beaudouin *et al*, 2002). In addition, the pEGFP vector containing the full-length LBR, designated as hLBR in pEGFP-N3, was provided by Dr Haraguchi (Haraguchi *et al*, 2000). A full-length HP1α cDNA was also amplified from the HEK293 cell cDNA library and was subcloned into pCMV–Myc (Clontech). For expression of JCV Agno, the cDNA was subcloned into either pGST–EGFP.pcDNA4HisMax (GST: glutathione-*S*-transferase) or pcDNA4/TO/Myc–His (Invitrogen, Carlsbad, CA, USA).

FRAP analysis. We performed the FRAP analysis according to Ellenberg *et al* (1997) and Scott & O'Hare (2001), with several technical modifications, because the performance of our laser scanning microscope (LSM) system was different from the LSM systems that they used. As the laser intensity of our LSM system was much lower than their system, our bleaching time was longer than their experiments. FRAP analysis of 293AG cells stably expressing LBR–EGFP was performed with the Olympus FV300 confocal microscope fitted with a ×60 oil-immersion objective (numerical aperture, 1.25). The cells (2×10^5) were plated on 35-mm dishes coated with type I collagen and were incubated with or without Dox for 24 h before analysis. Images were recorded at 488 nm (at 3% power) and an intense pulse of laser light (100% power) was then applied for 30 s to bleach the

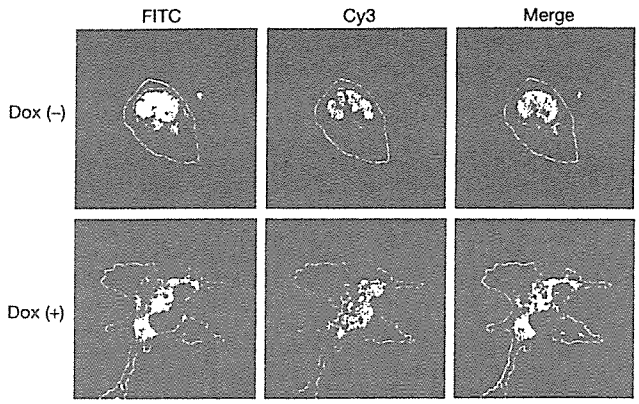

Fig 5 | Agno facilitates the nuclear egress of VLPs. The nuclei of Dox-treated (lower panels) or untreated (upper panels) 293AG cells were microinjected with VLPs and Cy3 (injection site marker; red fluorescence), and, after 1 h, the cells were subjected to immunofluorescence analysis with anti-VP1 (green). Blue lines indicate the rim of the nuclei and white lines indicate the edge of the cytoplasm.

fluorescent molecules in a defined region (2 × 2 μm). Recovery of fluorescence was monitored at 30 s intervals for 10 min by scanning with attenuated laser light (3% power). The FV300 software was used to generate a time series from the images and to plot the pixel intensity in the defined regions of interest for the duration of the experiment. At each time point, the intensity of an equivalent background area was subtracted and values were normalized for total loss of fluorescence. The relative recovery of fluorescence intensity was calculated as 100% × ((intensity at the recovery plateau)−(intensity at 1 min after bleaching))/((average intensity of the bleached region before bleaching)−(intensity at 1 min after bleaching)). We also subjected the pEGFP vector containing the full-length LBR (provided by Dr Haraguchi) to the FRAP analyses (Haraguchi *et al*, 2000).

Supplementary information is available at *EMBO reports* online (http://www.emboreports.org).

ACKNOWLEDGEMENTS

We thank M. Satoh and M. Sasada for technical assistance; A. Kihara, M. Matsuda and N. Mochizuki for helpful suggestions; and T. Haraguchi for the hLBR in pEGFP-N3 plasmid. Y.O. is a research fellow of the Japan Society for the Promotion of Science. This study was supported in part by grants from the Ministry of Education, Science, Technology, Sports, and Culture of Japan, the Ministry of Health, Labor, and Welfare of Japan, the Japan Human Science Foundation.

REFERENCES

Beaudouin J, Gerlich D, Daigle N, Eils R, Ellenberg J (2002) Nuclear envelope breakdown proceeds by microtubule-induced tearing of the lamina. *Cell* **108:** 83–96

Darbinyan A, Siddiqui KM, Slonina D, Darbinian N, Amini S, White MK, Khalili K (2004) Role of JC virus agnoprotein in DNA repair. *J Virol* **78:** 8593–8600

Ellenberg J, Siggia ED, Moreira JE, Smith CL, Presley JF, Worman HJ, Lippincott-Schwartz J (1997) Nuclear membrane dynamics and reassembly in living cells: targeting of an inner nuclear membrane protein in interphase and mitosis. *J Cell Biol* **138:** 1193–1206

Gerlich D, Beaudouin J, Gebhard M, Ellenberg J, Eils R (2001) Four-dimensional imaging and quantitative reconstruction to analyse complex spatiotemporal processes in live cells. *Nat Cell Biol* **3:** 852–855

Goldmann C *et al* (1999) Molecular cloning and expression of major structural protein VP1 of the human polyomavirus JC virus: formation of virus-like particles useful for immunological and therapeutic studies. *J Virol* **73:** 4465–4469

Haraguchi T, Koujin T, Hayakawa T, Kaneda T, Tsutsumi C, Imamoto N, Akazawa C, Sukegawa J, Yoneda Y, Hiraoka Y (2000) Live fluorescence imaging reveals early recruitment of emerin, LBR, RanBP2, and Nup153 to reforming functional nuclear envelopes. *J Cell Sci* **113:** 779–794

Komagome R, Sawa H, Suzuki T, Suzuki Y, Tanaka S, Atwood WJ, Nagashima K (2002) Oligosaccharides as receptors for JC virus. *J Virol* **76:** 12992–13000

Mazlo M, Ressetar HG, Stoner GL (2001) The neuropathology and pathogenesis of progressive multifocal leukoencephalopathy. *Hum Polyomaviruses: Mol and Clin Perspect* 257–335

Minc E, Allory Y, Worman HJ, Courvalin JC, Buendia B (1999) Localization and phosphorylation of HP1 proteins during the cell cycle in mammalian cells. *Chromosoma* **108:** 220–234

Muranyi W, Haas J, Wagner M, Krohne G, Koszinowski UH (2002) Cytomegalovirus recruitment of cellular kinases to dissolve the nuclear lamina. *Science* **297:** 854–857

Okada Y, Endo S, Takahashi H, Sawa H, Umemura T, Nagashima K (2001) Distribution and function of JCV agnoprotein. *J Neurovirol* **7:** 302–306

Okada Y, Sawa H, Endo S, Orba Y, Umemura T, Nishihara H, Stan AC, Tanaka S, Takahashi H, Nagashima K (2002) Expression of JC virus agnoprotein in progressive multifocal leukoencephalopathy brain. *Acta Neuropathol (Berl)* **104:** 130–136

Orba Y, Sawa H, Iwata H, Tanaka S, Nagashima K (2004) Inhibition of virus production in JC virus-infected cells by postinfection RNA interference. *J Virol* **78:** 7270–7273

Pante N, Kann M (2002) Nuclear pore complex is able to transport macromolecules with diameters of about 39 nm. *Mol Biol Cell* **13:** 425–434

Qu Q, Sawa H, Suzuki T, Semba S, Henmi C, Okada Y, Tsuda M, Tanaka S, Atwood WJ, Nagashima K (2004) Nuclear entry mechanism of the human polyomavirus JC virus-like particle: role of importins and the nuclear pore complex. *J Biol Chem* **279:** 27735–27742

Resnick J, Shenk T (1986) Simian virus 40 agnoprotein facilitates normal nuclear location of the major capsid polypeptide and cell-to-cell spread of virus. *J Virol* **60:** 1098–1106

Salina D, Bodoor K, Enarson P, Raharjo WH, Burke B (2001) Nuclear envelope dynamics. *Biochem Cell Biol* **79:** 533–542

Scott ES, O'Hare P (2001) Fate of the inner nuclear membrane protein lamin B receptor and nuclear lamins in herpes simplex virus type 1 infection. *J Virol* **75:** 8818–8830

Suzuki S, Sawa H, Komagome R, Orba Y, Yamada M, Okada Y, Ishida Y, Nishihara H, Tanaka S, Nagashima K (2001) Broad distribution of the JC virus receptor contrasts with a marked cellular restriction of virus replication. *Virology* **286:** 100–112

Ye Q, Worman HJ (1994) Primary structure analysis and lamin B and DNA binding of human LBR, an integral protein of the nuclear envelope inner membrane. *J Biol Chem* **269:** 11306–11311

Ye Q, Worman HJ (1996) Interaction between an integral protein of the nuclear envelope inner membrane and human chromodomain proteins homologous to *Drosophila* HP1. *J Biol Chem* **271:** 14653–14656

Ye Q, Callebaut I, Pezhman A, Courvalin JC, Worman HJ (1997) Domain-specific interactions of human HP1-type chromodomain proteins and inner nuclear membrane protein LBR. *J Biol Chem* **272:** 14983–14989

THE JOURNAL OF BIOLOGICAL CHEMISTRY
Vol. 280, No. 26, Issue of July 1, pp. 24948–24956, 2005
Printed in U.S.A.

Identification of FEZ1 as a Protein That Interacts with JC Virus Agnoprotein and Microtubules

ROLE OF AGNOPROTEIN-INDUCED DISSOCIATION OF FEZ1 FROM MICROTUBULES IN VIRAL PROPAGATION*

Received for publication, October 8, 2004, and in revised form, April 19, 2005
Published, JBC Papers in Press, April 20, 2005, DOI 10.1074/jbc.M411499200

Tadaki Suzuki‡, Yuki Okada‡ ‡‡, Shingo Semba‡§, Yasuko Orba‡ ‡‡, Satoko Yamanouchi‡, Shuichi Endo‡, Shinya Tanaka‡, Toshitsugu Fujita¶, Shun'ichi Kuroda¶, Kazuo Nagashima‡, and Hirofumi Sawa§‖**

From the ‡Laboratory of Molecular and Cellular Pathology, School of Medicine, Core Research for Evolutional Science and Technology, Japan Science and Technology Agency, the §21st Century Centers of Excellence Program for Zoonosis Control, and the ‖Department of Molecular Biology and Diagnosis, Research Center for Zoonosis Control, Hokkaido University, Sapporo 060-8638 and the ¶Department of Structural Molecular Biology, Institute of Scientific and Industrial Research (Sanken), Osaka University, Osaka 567-0047, Japan

The human polyomavirus JC virus (JCV) is the causative agent of a fatal demyelinating disease, progressive multifocal leukoencephalopathy, and encodes six major proteins, including agnoprotein. Agnoprotein colocalizes with microtubules in JCV-infected cells, but its function is not fully understood. We have now identified fasciculation and elongation protein zeta 1 (FEZ1) as a protein that interacted with JCV agnoprotein in a yeast two-hybrid screen of a human brain cDNA library. An *in vitro* binding assay showed that agnoprotein interacted directly with FEZ1 and microtubules. A microtubule cosedimentation assay revealed that FEZ1 also associates with microtubules and that agnoprotein induces the dissociation of FEZ1 from microtubules. Agnoprotein inhibited the promotion by FEZ1 of neurite outgrowth in PC12 cells. Conversely, overexpression of FEZ1 suppressed JCV protein expression and intracellular trafficking in JCV-infected cells. These results suggest that FEZ1 promotes neurite extension through its interaction with microtubules, and that agnoprotein facilitates JCV propagation by inducing the dissociation of FEZ1 from microtubules.

The human polyomavirus JC virus (JCV)[1] is the causative agent of progressive multifocal leukoencephalopathy, a fatal demyelinating disease. The genome of JCV comprises a double-stranded circular DNA molecule that contains three functional regions: the viral early and late genes and the noncoding regulatory sequence (1). The early region of the JCV genome encodes the large T and small t antigens, which are responsible for the initiation of viral DNA replication and activation of late gene transcription (2–4). The late coding region encodes three structural proteins (VP1, VP2, and VP3) that are components of the viral capsid (5). In addition, the leader sequence of late transcripts encodes agnoprotein, a viral auxiliary protein that contains 71 amino acids (6).

The auxiliary proteins of various eukaryotic viruses have diverse effects on different stages of infection, including transcription (7, 8), viral assembly (9), and the release of viral particles (10, 11). They can also affect host cell functions and thereby contribute to the pathogenesis of viral-induced disease (12). The agnoprotein of simian vacuolating virus 40 (SV40), which belongs to the same polyomavirus family as does JCV, contributes to various stages of the viral lytic cycle. Mutation of the agnoprotein of SV40 was found to result in a moderate growth defect that was attributable to impairment of the viral maturation pathway (13–15). Immunofluorescence analysis revealed that SV40 agnoprotein facilitates the localization of VP1, the major capsid protein, to the nucleus and perinuclear region of infected cells (16). Furthermore, the lack of agnoprotein led to inefficient release of mature SV40 virions from infected cells and impaired the ability of the virus to propagate in monkeys (14).

In addition to SV40, JCV is closely related to other polyomaviruses, including human BK virus. These viruses exhibit marked nucleotide sequence similarity, especially in the coding regions (1). All JCV proteins with the exception of agnoprotein are localized predominantly in the nuclei of infected cells (17, 18), whereas JCV agnoprotein is largely restricted to the perinuclear region of the cytoplasm (19), as is SV40 agnoprotein (20). We previously showed that deletion of the agnogene of JCV results in a viral growth defect (21). Furthermore, a small interfering RNA (siRNA) specific for agnoprotein mRNA was found to inhibit JCV infection (22). These observations suggest that the agnoprotein of JCV, like that of SV40, plays an important role in viral propagation, although the molecular mechanism of this action remains unknown.

We have now identified fasciculation and elongation protein zeta 1 (FEZ1) as a protein that interacted with JCV agnoprotein in a yeast-two hybrid assay. FEZ1 is a brain-specific coiled-

* This work was supported in part by grants from the Ministry of Education, Science, Technology, Sports, and Culture of Japan, the Ministry of Health, Labor, and Welfare of Japan, the Japan Human Science Foundation. The costs of publication of this article were defrayed in part by the payment of page charges. This article must therefore be hereby marked "*advertisement*" in accordance with 18 U.S.C. Section 1734 solely to indicate this fact.

** To whom correspondence should be addressed: Dept. of Molecular Biology and Diagnosis, Hokakido University Research Center for Zoonosis Control, N15, W7, Kita-ku, Sapporo 060-8638, Japan. Tel.: 81-11-706-5053; Fax: 81-11-706-7806; E-mail: h-sawa@patho2.med.hokudai.ac.jp.

‡‡ Research fellows of the Japan Society for the Promotion of Science.

[1] The abbreviations used are: JCV, JC virus; FEZ1, fasciculation and elongation protein zeta 1; GST, glutathione *S*-transferase; GFP, green fluorescent protein; PMSF, phenylmethylsulfonyl fluoride; PBS, phosphate-buffered saline; NGF, nerve growth factor; RT, reverse transcription; CC coiled-coil; Dox, doxycycline; PKC, protein kinase C; siRNA, small interfering RNA; PIPES, piperazine-*N*,*N*′-bis(2-ethanesulfonic acid); His-Agno, histidine-tagged agnoprotein; MES, 4-morpholineethanesulfonic acid.

coil protein that comprises 392-amino acid residues and is expressed in neurons (23). It is related to *Caenorhabditis elegans* UNC-76, which is required for normal axonal bundling and outgrowth. We further demonstrate that agnoprotein inhibited the function of FEZ1 apparently by blocking the association of FEZ1 with microtubules, and overexpression of FEZ1 inhibited the intracellular spread of JCV. Our results suggest that agnoprotein promotes the intracellular translocation of viral particles on microtubules by inducing the dissociation of FEZ1.

EXPERIMENTAL PROCEDURES

Construction of Plasmids—A full-length FEZ1 cDNA was amplified by the PCR from an adult human brain cDNA library and was subcloned into pCXN2-FLAG (24), pGEX6P1 (Amersham Biosciences), and pEGFP-N1 (Clontech, Palo Alto, CA); the resulting expression vectors were designated pFLAG-FEZ1 (for expression of FEZ1 with an NH_2-terminal FLAG tag), pGST-FEZ1 (for expression of FEZ1 fused at its NH_2 terminus with glutathione *S*-transferase), and pFEZ1-GFP (for expression of FEZ1 fused at its COOH terminus to green fluorescent protein), respectively. Complementary DNAs for deletion mutants of FEZ1 were generated by PCR from pFLAG-FEZ1 and subcloned into pGEX6P1. For expression of JCV agnoprotein in mammalian cells, the agnoprotein cDNA was amplified by PCR from a plasmid containing the JCV genome, pJC1->4pJCV (HSRRB, Osaka, Japan), and subcloned into either pcDNA4HisMax (Invitrogen) or the bicistronic expression vector pERedNLS (kindly provided by M. Matsuda).

Yeast Two-hybrid Assay—The yeast two-hybrid assay was performed with a Matchmaker System 3 and an adult human brain cDNA library obtained from Clontech. Yeast AH109 cells were transformed with both the brain cDNA library and a full-length cDNA for JCV agnoprotein subcloned into the yeast shuttle vector pGBKT7. Plasmids isolated from positive colonies were introduced into *Escherichia coli* DH5α and sequenced, and the DNA sequence data were compared with sequences in the NCBI data base with the BLAST program.

Cell Culture and Virus Preparation—Human embryonic kidney 293 (HEK293) cells (HSRRB), SV40-transformed human glial SVG-A cells (kindly provided by W. J. Atwood) (25), and JCV-producing (JCI) cells (26) were maintained under an atmosphere of 5% CO_2 at 37 °C in Dulbecco's minimal essential medium supplemented with 10% heat-inactivated fetal bovine serum, 2 mM L-glutamine, penicillin, and streptomycin (Sigma). HEK293 cells that express JCV agnoprotein in an inducible manner (293AG cells) were established with the T-REx system (Invitrogen); agnoprotein expression was induced by exposure of the cells to doxycycline (Invitrogen) at a final concentration of 1 μg/ml. To establish 293AG cells that stably express FEZ1-GFP, we transfected 293AG cells with pFEZ1-GFP and cultured the transfectants in the presence of Geneticin (Invitrogen) at 400 μg/ml. Several clones were expanded in the selection medium, after which expression of FEZ1-GFP was confirmed by immunoblot analysis. Control 293AG cell lines were similarly established by stable transfection with pEGFP-N1. To establish SVG-A cells that stably express FLAG-FEZ1, we transfected SVG-A cells with pFLAG-FEZ1 and cultured the transfectants in the presence of Geneticin (100 μg/ml). Expression of FLAG-FEZ1 in selected cells was confirmed by immunoblot analysis. Again, control SVG-A cell lines were similarly established by stable transfection with pCXN2-FLAG. PC12 cells stably expressing either FEZ1-GFP or GFP were kindly provided by T. Fujita (27) and were maintained in Dulbecco's minimal essential medium supplemented with 10% heat-inactivated fetal bovine serum, 2 mM L-glutamine, penicillin, streptomycin, and Geneticin (400 μg/ml). For virus preparation, JC virus-infected SVG-A cells were cultured for 2 weeks, harvested, and suspended in 10 mM Tris-HCl (pH 7.5) containing 0.2% bovine serum albumin. The cells were frozen and thawed three times and then treated for 16 h at 37 °C with neuraminidase type V (Sigma) at 0.05 unit/ml. After an additional incubation for 30 min at 56 °C, the cell lysate was centrifuged at 1000 × *g* for 10 min, and the resulting supernatant was assayed for JCV by a hemagglutination assay (28) and stored at −80 °C until use.

Protein Preparation—Recombinant baculovirus bearing Agno was constructed using the Gateway system (Invitrogen). Briefly, the coding region of Agno was amplified by PCR using a specific primer set 5′-GGGGACAAGTTTGTACAAAAAAGCAGGCTGGATGGTTCTTCCGCCAGCTGTC-3′ and 5′-GGGGACCACTTTGTACAAGAAAGCTGGGTCTATGTAGCTTTTGGTTCA-3′ and pBR-Mad1 (30) as a template. PCR products were subcloned into pDONR201 (Invitrogen), following cloning into pDEST10 (Invitrogen). Recombinant baculoviruses were prepared according to manufacturer's instruction. The histidine-tagged agnoprotein (His-Agno) was purified as follows: a 500-ml culture of Sf9 cells infected with the recombinant baculovirus for 3 days was harvested by centrifugation at 500 × *g* for 10 min, and the cell pellet was resuspended in 5 volumes of the lysis buffer (600 mM NaCl, 20 mM Tris-HCl, pH 7.5, 0.5% (v/v) Triton X-100, 1 mM PMSF, and 0.05 mg/ml DNase) using the Teflon homogenizer. After rotation for 30 min at 4 °C, the extract was clarified by centrifugation at 24,000 × *g* for 20 min at 4 °C. The supernatant was loaded onto the nickel-chelated Cellulofine (Seikagaku Corp., Tokyo, Japan) column pre-equilibrated with the lysis buffer without PMSF and DNase, and the column was washed with same buffer. After extensively washing with the solution (600 mM NaCl, 20 mM imidazole-HCl, pH 7.5), the bound proteins were eluted with the buffer (600 mM NaCl and 200 mM imidazole-HCl, pH 7.5). The anti-Agno antibody-conjugated Sepharose resin was added into the eluate, and the mixture was rotated overnight at 4 °C. The resin was transferred into an empty column and washed with TBS containing 0.05% (w/v) Tween 20 (TBST). The bound proteins were eluted with the solution (0.1 M glycine-HCl, pH 2.8), and the elute was immediately neutralized by addition of 0.1 volume of 1 M Tris-base. The fractions containing His-Agno were pooled and dialyzed against TBS. The purified His-Agno was stored at 4 °C until use.

Primary Antibodies—Mouse monoclonal antibodies to large T antigen (Ab-2), to α-tubulin, to pan-actin (MAB1501R), and to MAP2 (clone AP-20) were obtained from Oncogene Research Products (Uniondale, NY), Sigma, Chemicon International (Temecula, CA), and Roche Diagnostics, respectively. Goat polyclonal antibodies to GST were from Amersham Biosciences. Rabbit polyclonal antibodies to JCV agnoprotein and to JCV VP1 were produced as described previously (19, 29). Rabbit polyclonal antibodies to enhanced GFP were kindly provided by N. Mochizuki. Mouse monoclonal antibodies to FLAG (M2) and horseradish peroxidase-conjugated mouse monoclonal antibodies to FLAG (M2) were from Sigma.

Transfection, Immunoblot Analysis, and Immunoprecipitation—Cell transfection was performed with Lipofectamine 2000 (Invitrogen). For immunoblot analysis, cells were harvested 24–48 h after transfection, lysed in radioimmune precipitation assay buffer (10 mM Tris-HCl (pH 7.5), 150 mM NaCl, 5 mM EDTA, 50 mM NaF, 10% glycerol, 1% Triton X-100, 1% sodium deoxycholate, 0.1% SDS, 0.5 mM phenylmethylsulfonyl fluoride (PMSF)), and mixed with Complete protease inhibitor mixture (Roche Diagnostics) (30). The cell lysates were fractionated by SDS-polyacrylamide gel electrophoresis, and the separated proteins were transferred to a polyvinylidene difluoride filter (Millipore, Bedford, MA). The filter was incubated with primary antibodies, and immune complexes were then detected with horseradish peroxidase-conjugated secondary antibodies and ECL reagents (Amersham Biosciences). The FLAG epitope was detected directly with horseradish peroxidase-conjugated primary antibodies.

For detection of *in vivo* interaction between agnoprotein and FEZ1, 293AG cells were transfected with pFLAG-FEZ1, and, 48 h after transfection, lysed in buffer C (50 mM Hepes-KOH (pH 7.8), 420 mM KCl, 0.1 mM EDTA, 0.05% Triton X-100, 5 mM PMSF), mixed with Complete protease inhibitor mixture, and subjected to immunoprecipitation. For detection of *in vivo* interaction between FEZ1 and tubulin, 293AG cells stably expressing FEZ1-GFP were lysed in PTN buffer (100 mM PIPES-NaOH (pH 6.3), 30 mM Tris-HCl, 50 mM NaCl, 1 mM EGTA, 1.25 mM EDTA, 1 mM dithiothreitol, 1% Triton X-100, 10 mM PMSF), mixed with Complete protease inhibitor mixture, and subjected to immunoprecipitation.

Immunoprecipitation was performed by incubation of cell lysates at 4 °C first for 1 h with protein G-Sepharose FF beads (Amersham Biosciences) and then, after removal of the beads, for 4 h with antibody-coupled protein G-Sepharose FF beads. After washing with cell lysis buffer, the bead-bound proteins were subjected to immunoblot analysis.

Immunofluorescence Analysis—Cells were fixed with 3% paraformaldehyde in phosphate-buffered saline (PBS), permeabilized with 0.1% Triton X-100 in PBS, and incubated at room temperature with 5% dried skim milk in PBS (31). For detergent extraction, cells were washed once with PBS and twice with PHEM buffer (60 mM PIPES, 25 mM HEPES, pH 6.9; 10 mM EGTA, 2 mM $MgCl_2$) before extraction with 0.2% Saponin in PHEM buffer for 3 min on ice. The detergent-insoluble cell components remaining on the coverslips were then washed with PHEM buffer and fixed with methanol for 4 min at −20 °C. The cells were then incubated first with primary antibodies and then with Alexa 488- or Alexa 594-labeled goat antibodies to rabbit immunoglobulin G or with Alexa 594-labeled goat antibodies to mouse immunoglobulin G (Molecular Probes, Eugene, OR). Nuclei were counterstained with propidium iodide (0.2 μg/ml), and the cells

were then observed with a confocal laser-scanning microscope (Olympus, Tokyo, Japan).

GST Precipitation Assay—GST fusion proteins of FEZ1 or its deletion mutants were expressed in *Escherichia coli* AD494 DE3 and purified with the use of glutathione-Sepharose 4B beads (Amersham Pharmacia Biotech). For *in vitro* GST precipitation assays, GST or GST fusion proteins (50 pmol) were mixed with 10 μl of the histidine-tagged agnoprotein in a final volume of 500 μl with binding buffer (10 mM Tris-HCl (pH 7.4), 150 mM NaCl, 5 mM EDTA, 0.5% Nonidet P-40, and 0.5 mM PMSF) and Complete protease inhibitor mixture and then incubated for 1 h at 4 °C. After the addition of 10 μl of 50% (v/v) glutathione-Sepharose 4B, the mixture was incubated for another 3 h at 4 °C. The beads were separated by centrifugation and washed with binding buffer, and the bound proteins were subjected to immunoblot analysis with antibodies to agnoprotein.

Microtubule Cosedimentation Assay—Microtubule binding assays were performed as previously described (32–35). In brief, GST fusion proteins of FEZ1 or its deletion mutants (0.5 μg) in 50 μl of a MES-based buffer (100 mM MES-NaOH (pH 6.8), 1 mM EGTA, 0.1 mM EDTA, 0.5 mM $MgCl_2$, 1 mM dithiothreitol, 0.1 mM GTP) supplemented with 50 μM Taxol (Sigma) were centrifuged at 100,000 × *g* for 1 h at 25 °C. Purified tubulin (Sigma) at 5 mg/ml in the MES-based buffer was polymerized by incubation for 30 min at 37 °C in the presence of 50 μM Taxol and GFP at a final concentration of 2.5 mM, and the polymerized microtubules were separated by centrifugation at 100,000 × *g* for 30 min at 25 °C. The supernatants containing the GST fusion proteins were then incubated with the polymerized microtubules (50 μg) for 30 min at 37 °C, after which the mixtures were each layered on top of 100 μl of 30% sucrose in the MES-based buffer and centrifuged at 30,000 × *g* for 30 min at 25 °C. The resulting supernatants and pellets (washed once with the MES-based buffer) were subjected to immunoblot analysis.

For examination of the interaction between agnoprotein and microtubules, JCI cells were lysed in PTN buffer supplemented with Complete protease inhibitor mixture, and the cell lysate was centrifuged at 100,000 × *g* for 30 min at 25 °C. The resulting supernatant (60 μl containing 100 μg of protein) was added to a pellet of polymerized microtubules (50 μg) and incubated for 30 min at 37 °C in the presence of 50 μM Taxol. Samples were then layered over 100 μl of 30% sucrose in the MES-based buffer and centrifuged at 30,000 × *g* for 30 min at 25 °C. The resulting supernatants and pellets (washed once with the MES buffer) were subjected to immunoblot analysis.

Assay of Neurite Extension in PC12 Cells—PC12 cells stably expressing either FEZ1-GFP or GFP were transfected with pERedNLS-agno or the empty vector. At 24 h after transfection, the cells were incubated for 4 h in serum-free medium and then maintained for 48 h in serum-free medium supplemented with nerve growth factor (NGF) (Sigma) at a concentration of 50 ng/ml. The cells were washed with PBS, fixed with 3% paraformaldehyde at room temperature for 10 min, and then washed three times with PBS. Cells expressing agnoprotein were identified on the basis of their DsRed-positive nuclei. A change in cell morphology characterized by neurite outgrowth, cell flattening, and an increase in the size of the cell body was defined previously (27, 36, 37).

RT-PCR Analysis—For RNA extraction, cells grown in 6-well plates were washed once with PBS and harvested with trypsin-EDTA. Total RNA was isolated with the use of an RNeasy Mini kit (Qiagen, Valencia, CA), and portions (500 ng) were treated with 2 units of DNase I (Invitrogen) for 1 h at 37 °C in a 10-μl reaction mixture before incubation with 2.5 mM EDTA for 15 min at 65 °C. The treated RNA (4 μl) was subjected to RT with a Superscript first-strand synthesis system (Invitrogen). The absence of contamination with genomic DNA was verified by the addition of RNase-free water instead of Superscript II reverse transcriptase as a negative control for each sample. PCR was performed in a final volume of 50 μl containing cDNA, Gene *Taq* universal buffer, 2.5 mM of each deoxynucleoside triphosphate, Gene *Taq* polymerase (Nippon Gene, Tokyo, Japan), and primers specific either for FEZ1 (5′-CACTGGTGAGTCTGGATG-3′ and 5′-CGAGGTCCTCCATGGACTTGAAG-3′) or for β-actin (5′-TTGCCGACAGGATGCAGAA-3′ and 5′-GCCGATCCACACGGAGTACT-3′). The reaction mixtures were incubated at 94 °C for 1 min and then subjected to 38 cycles of 94 °C for 30 s, 56 °C for 30 s, and 72 °C for 30 s with a GeneAmp 5700 Sequence Detection System (Applied Biosystems, Foster City, CA). All reactions were confirmed in at least three independent experiments.

siRNA Preparation—The following stealth RNA duplexes were synthesized by Invitrogen: FEZ1–301 sense, 5′-GAGAAGCUCAAUGUCUGCUUUCGGA-3′ and antisense, 5′-UCCGAAAGCAGACAUUGAGCUUCUC-3′; FEZ1–352 sense, 5′-GCUCCCGUGAAGAACCAGUUACAGA-3′ and antisense, 5′-UCUGUAACUGGUUCUUCACGGGAGC-3′; Scramble sense, 5′-GCAUCGUACAGACAAUCUUCAGUUU-3′ and antisense, 5′-AAACTGAAGAUUGUCUGUACGAUGC-3′.

Virus Inoculation and siRNAs Transfection—SVG-A sells were grown to 50% confluence on a 6-well plate and incubated with 1000 hemagglutination units of JCV in Dulbecco's minimal essential medium containing 2% fetal bovine serum for 24 h, At 24 h post inoculation of JCV, transfection of siRNA (100 pmol) were performed with Lipofectamine 2000 (Invitrogen) to the JCV-infected SVG-A cells. The cells were harvested and analyzed by Western blot analysis at 96 h post transfection. The results were confirmed by at least three independent experiments.

RESULTS

Identification of FEZ1 as an Agnoprotein-binding Protein—We first performed a yeast two-hybrid assay with full-length JCV agnoprotein as the bait to identify proteins that interact with agnoprotein. Several positive clones were isolated from a human brain cDNA library and were found to encode a portion of FEZ1 that contains the three poly-glutamic acid regions and the coiled-coil (CC) domain (Fig. 1*A*). The largest cDNA clone encoded amino acids 32–392 of human FEZ1.

To examine the interaction between agnoprotein and FEZ1, we established a cell line, designated 293AG, that was derived from HEK293 cells and that expresses JCV agnoprotein (tagged with the hexahistidine and Myc epitopes at its NH_2 terminus) under the control of a tetracycline-responsive promoter. All 293AG cells expressed the recombinant agnoprotein (molecular size, ~14 kDa) within 3 h of exposure to doxycycline (Dox). In the absence of Dox, we failed to detect agnoprotein in the cells by immunoblot or immunocytofluorescence analysis (data not shown). Immunoprecipitation and immunoblot analysis of 293AG cells transfected with an expression vector for FLAG epitope-tagged FEZ1 revealed that FLAG-FEZ1 coprecipitated with agnoprotein (Fig. 1*B*).

The subcellular localization of exogenously expressed agnoprotein and FEZ1 in transfected HEK293 cells was examined by immunocytofluorescence analysis. Confocal microscopy revealed that agnoprotein immunoreactivity was present in the perinuclear region and extended into the cytoplasm in a mesh-like pattern (Fig. 1*C*). In most cells, FEZ1 was detected throughout the cytoplasm and colocalized with agnoprotein only in the perinuclear region (Fig. 1*C*, *upper panels*). However, in some cells the localization of FEZ1 is mirrored by that of agnoprotein and well colocalized with agnoprotein (Fig. 1*C*, *lower panels*). This suggests that FEZ1 was recruited to the same location as agnoprotein as a result of interactions between FEZ1 and agnoprotein.

Association of Agnoprotein with Microtubules—Agnoprotein colocalized with microtubules in the perinuclear region of JCV-infected SVG-A cells (Fig. 2*A*), consistent with our previous observations (38). To confirm the association between agnoprotein and microtubules, we performed a microtubule cosedimentation assay with lysates of JCI cells and microtubules polymerized in the presence of Taxol. Agnoprotein was indeed detected in the sedimented fraction only in the presence of microtubules (Fig. 2*B*). In contrast, the large T antigen of JCV, which was detected in the nucleus of JCV-infected cells (19), was present exclusively in the supernatant fraction even in the presence of microtubules (Fig. 2*B*), suggesting that the association of agnoprotein with microtubules is specific. However, it was not clear if agnoprotein binds directly to microtubules, because the cosedimentation assays were performed on cell extracts. To confirm the direct binding of agnoprotein to microtubules, we performed the assay using recombinant histidine-tagged agnoprotein (His-Agno) from the insect cells infected with the recombinant baculovirus encoding His-Agno cDNA (Fig. 2*C*). We incubated the His-Agno in the MES-based buffer in the absence (Fig. 2*D*, *lanes 1* and *6*) or presence of 40 μM

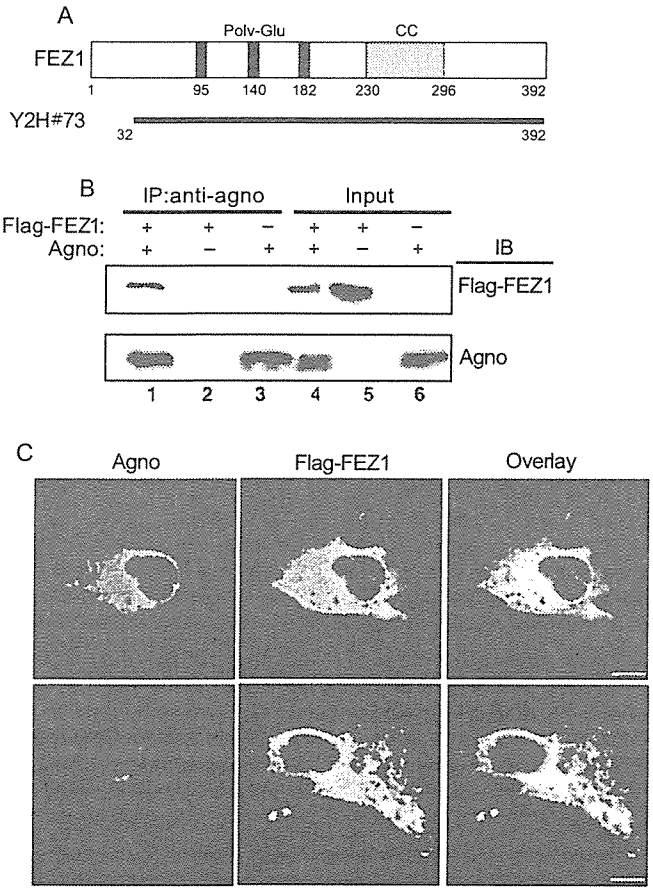

FIG. 1. **Interaction of JCV agnoprotein and FEZ1.** *A*, predicted structural organization of human FEZ1. FEZ1 contains three poly-Glu regions (*black rectangles*) and a CC domain (*gray rectangle*). The *black bar* indicates a FEZ1 clone (Y2H #73) isolated from a human brain cDNA library by a yeast two-hybrid assay with full-length JCV agnoprotein as the bait. *B*, interaction of agnoprotein with FEZ1 in mammalian cells. 293AG cells were transfected with pFLAG-FEZ1 (*lanes 1, 2, 4,* and *5*) or with the corresponding empty vector (*lanes 3* and *6*), and were subsequently incubated in the absence (*lanes 2* and *5*) or presence (*lanes 1, 3, 4,* and *6*) of Dox for 24 h. Cell lysates were then subjected to immunoprecipitation (*IP*) with antibodies to agnoprotein (*anti-agno*), and the resulting precipitates were subjected to immunoblot analysis (*IB*) with antibodies to FLAG or to agnoprotein, as indicated (*lanes 1–3*). A portion of cell lysates corresponding to 2% of the input for immunoprecipitation was also subjected directly to immunoblot analysis with the same antibodies (*lanes 4–6*). *C*, intracellular localization of recombinant agnoprotein and FLAG-FEZ1. HEK293 cells were transfected with pFLAG-FEZ1 and pcDNA4HisMax-agnoprotein. Forty-eight hours after transfection, the cells were stained with antibodies to agnoprotein (*red, left*) and to FLAG (*green, center*). The merged fluorescence images (*Overlay, right*) are also shown. *Scale bars*, 10 μm.

nocodazole (*lanes 2* and *7*) or 20 μM Taxol (*lanes 3* and *8*) or 40 μM nocodazole-treated microtubules (*lanes 4* and *9*) or 20 μM Taxol-treated microtubules (*lane 5* and *10*). In the absence of polymerized microtubules, agnoprotein remains in the supernatant fraction (*lanes 1–3*). Only small amounts of agnoprotein were detected in the sedimented fraction in the presence of nocodazole-treated microtubules (*lane 9*), whereas a significant amount of agnoprotein associated with microtubule pellets in the presence of Taxol-polymerized microtubules (*lane 10*). These results demonstrate that agnoprotein binds directly to microtubules. To examine if agnoprotein colocalizes specifically with microtubules, JCV-infected cells (JCI cells) were treated with either cytochalasin D, which specifically depolymerizes actin fibers, or nocodazole, which depolymerizes microtubules (Fig. 2*E*). In cells treated with Me_2SO or cytochalasin D, agnoprotein was still localized in the perinuclear region and cytoplasm. In cells treated with nocodazole, however, agnoprotein was found in aggregates dispersed throughout the remainder of the cell. These observations suggest that agnoprotein colocalizes specifically with microtubules.

Agnoprotein-induced Dissociation of FEZ1 from Microtubules—We next examined whether a GST fusion protein of full-length FEZ1 interacted with microtubules in the microtubule cosedimentation assay. GST-FEZ1, but not GST, was detected in the sedimented fraction in the presence of polymerized microtubules (Fig. 3*A*). In addition, both α-tubulin and agnoprotein were detected in immunoprecipitates prepared with antibodies to GFP from lysates of Dox-treated 293AG cells expressing a FEZ1-GFP fusion protein (Fig. 3*B*). Together, these data suggested that FEZ1 directly interacts with microtubules.

To examine whether agnoprotein affects the interaction of FEZ1 with microtubules, we performed the microtubule cosedimentation assay with lysates of 293AG cells stably expressing FEZ1-GFP. The expression level of agnoprotein in the cells was varied by their incubation with Dox for 0, 3, 6, 12, or 24 h. The amount of FEZ1-GFP that cosedimented with microtubules decreased as the expression level of agnoprotein increased (Fig. 3*C*). Conversely, the amount of agnoprotein that precipitated with microtubules increased in a concentration-dependent manner. However, the amount of MAP2 that cosedimented with microtubules did not change. These observations suggested that agnoprotein induces the dissociation of FEZ1 from microtubules, and that competition is specific between agnoprotein and FEZ1.

Regions of FEZ1 That Mediate Interaction with Microtubules and Agnoprotein—To identify the region of FEZ1 that mediates its interaction with agnoprotein, we constructed a series of deletion mutants of FEZ1 as GST fusion proteins (Fig. 4, *A* and *B*) and subjected them to GST precipitation assays. The deletion mutants of FEZ1 fused to GST were incubated with purified the histidine-tagged agnoprotein (His-Agno) expressed in insect cells and then precipitated with glutathione-Sepharose beads. Immunoblot analysis of bead-bound proteins revealed that wild-type FEZ1 and the deletion mutant of FEZ1 containing residues 192–392 (C192) interacted with agnoprotein to similar extents, whereas the deletion mutant of FEZ1 containing residues 163–296 (N296) precipitated progressively smaller amounts of agnoprotein, and no binding was observed with the COOH-terminal deletion mutant containing residues 1–191 (N191) and an NH_2-terminal deletion mutant containing residues 297–392 (C297) (Fig. 4*C*). These observations suggested that agnoprotein binds directly to FEZ1, and the CC domain of FEZ1 is important for the association with agnoprotein.

We next attempted to delineate the region of FEZ1 responsible for association with microtubules. The deletion mutants of FEZ1 fused to GST were subjected to a microtubules cosedimentation assay. The FEZ1 C192 and FEZ1 C297 mutants retained the ability to bind to microtubules (Fig. 4*D*). In contrast, the FEZ1 N191 mutant failed to interact with microtubules. The FEZ1 N296 mutant detected in sedimented fraction in the absence of microtubules as well as presence of microtubules, showing that the FEZ1 N296 mutant could sediment by itself independently with microtubules. These results suggested that the COOH-terminal region (residues 297–392) of FEZ1 contribute to the interaction with microtubules.

Thus, we have demonstrated that the binding regions of agnoprotein and microtubules with FEZ1 did not overlap each other. To further investigate the mechanism how agnoprotein disrupts the interaction between FEZ1 and microtubules, we performed a GST precipitation assay using GST-fused FEZ1 proteins and cell lysates from the agnoprotein-inducible cell line (293AG cells). This demonstrated that precipitated α-tu-

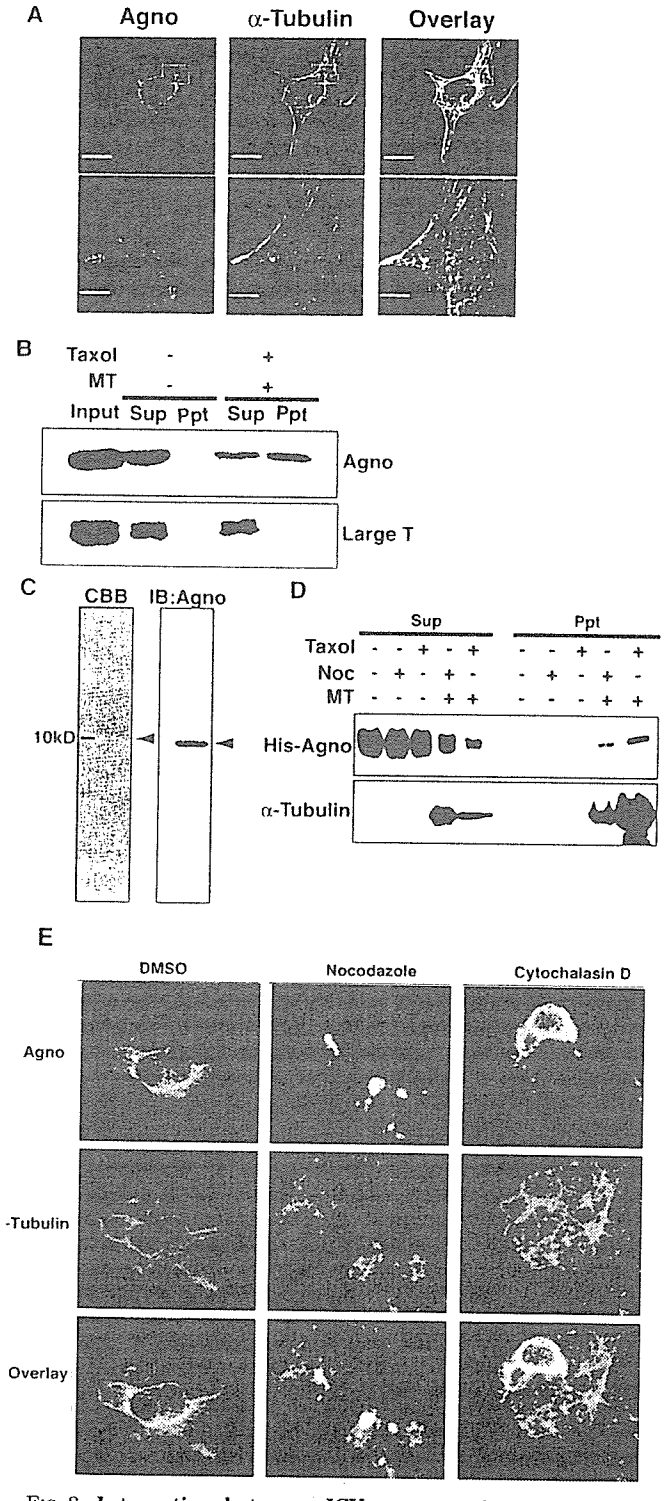

FIG. 2. **Interaction between JCV agnoprotein and microtubules.** *A*, intracellular localization of agnoprotein (*red*, *left*) and α-tubulin (*green*, *center*) in JCV-infected SVG-A cells. The merged fluorescence images (*Overlay*, *right*) are also shown. The cells were examined 7 days after inoculation with JCV (1,000 hemagglutination units per 1×10^6 cells). *Enlarged dotted rectangles* of the images are represented in the *lower panels*. *Scale bars*, 20 μm (*upper panels*) and 5 μm (*lower panels*). *B*, microtubule cosedimentation assay with a lysate of JCV-infected SVG-A cells. Cell lysate was incubated in the absence (−) or presence (+) of microtubules (*Mt*) and Taxol (*Taxol*), after which the precipitates (*Ppt*) and supernatants (*Sup*) obtained by centrifugation of the incubation mixtures were subjected to immunoblot analysis with antibodies to agnoprotein and to JCV large T antigen. A portion of the cell lysate corresponding to 10% of the input to the sedimentation assay was also subjected directly to immunoblot analysis with the same antibodies. *C*, the purified histidine-tagged agnoprotein (*arrowhead*).

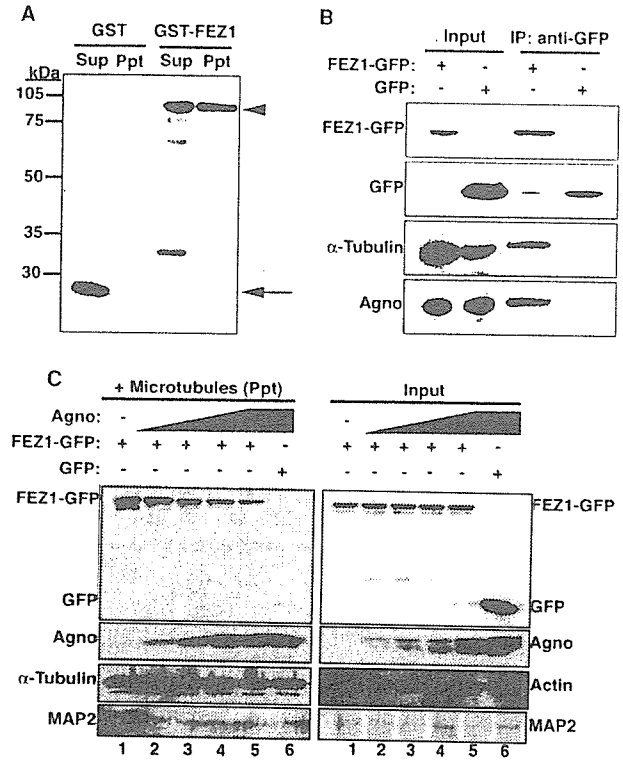

FIG. 3. **Agnoprotein-sensitive interaction of FEZ1 with microtubules.** *A*, microtubule cosedimentation assay performed with GST or GST-FEZ1. The recombinant proteins were incubated with microtubules, after which the precipitates and supernatants of the incubation mixtures were subjected to immunoblot analysis with antibodies to GST. The positions of GST-FEZ1 (*arrowhead*) and GST (*arrow*) are indicated. *B*, coprecipitation of α-tubulin and agnoprotein with FEZ1-GFP. 293AG cells stably expressing FEZ1-GFP or GFP were incubated with Dox (for 24 h), lysed, and subjected to immunoprecipitation with antibodies to GFP, and the resulting precipitates were subjected to immunoblot analysis with antibodies to GFP, to α-tubulin, and to agnoprotein. A portion of the cell lysates corresponding to 5% of the input for immunoprecipitation was also subjected directly to immunoblot analysis with the same antibodies. *C*, agnoprotein-induced dissociation of FEZ1 from microtubules. 293AG cells stably expressing FEZ1-GFP (*lanes 1–5*) or GFP (*lanes 6*) were incubated with Dox for 0 h (*lanes 1*), 3 h (*lanes 2*), 6 h (*lanes 3*), 12 h (*lanes 4*), or 24 h (*lanes 5* and *6*) and were then subjected to the microtubule cosedimentation assay. The microtubule precipitates (*left panel*) as well as a portion of the cell lysates corresponding to 10% of the input to the sedimentation assay (*right panel*) were subjected to immunoblot analysis with antibodies to GFP, to agnoprotein, to MAP2, and either to α-tubulin or to actin.

bulin with wild type FEZ1 or FEZ1 C192 mutant were remarkably attenuated in the presence of agnoprotein; however, precipitated α-tubulin with FEZ1 C297 mutant lacking the agnoprotein binding site was not altered even in the presence of

20 μl of sample was subjected to SDS-PAGE and CBB staining (*left panel*), immunoblot analysis (*right panel*). *D*, microtubule cosedimentation assay with the purified histidine-tagged agnoprotein (*His-Agno*). His-Agno was incubated in the absence (*lanes 1* and *6*) or presence of 40 μM nocodazole (*lanes 2* and *7*) or 20 μM Taxol (*lanes 3* and *8*) or 40 μM nocodazole-treated microtubules (*lanes 4* and *9*) or 20 μM Taxol-treated microtubules (*lanes 5* and *10*), after which the precipitates (*Ppt*) and supernatants (*Sup*) obtained by centrifugation of the incubation mixtures were subjected to immunoblot analysis with antibodies to agnoprotein and to α-tubulin. *E*, effect of nocodazole and cytochalasin D on the localization of agnoprotein in JCV-infected cells. JCI cells in absence of drugs (Me_2SO (*DMSO*), *left*) or treated with 4 μM nocodazole (*center*) or 0.5 μM cytochalasin D (*right*) were incubated for 2 h at 37 °C. The cells were extracted with 0.2% saponin, fixed, and analyzed by double immunofluorescence with anti-agnoprotein antibody (*green*, *upper*) and anti-α-tubulin antibody (*red*, *middle*). The merged fluorescence images (*Overlay*) are also shown.

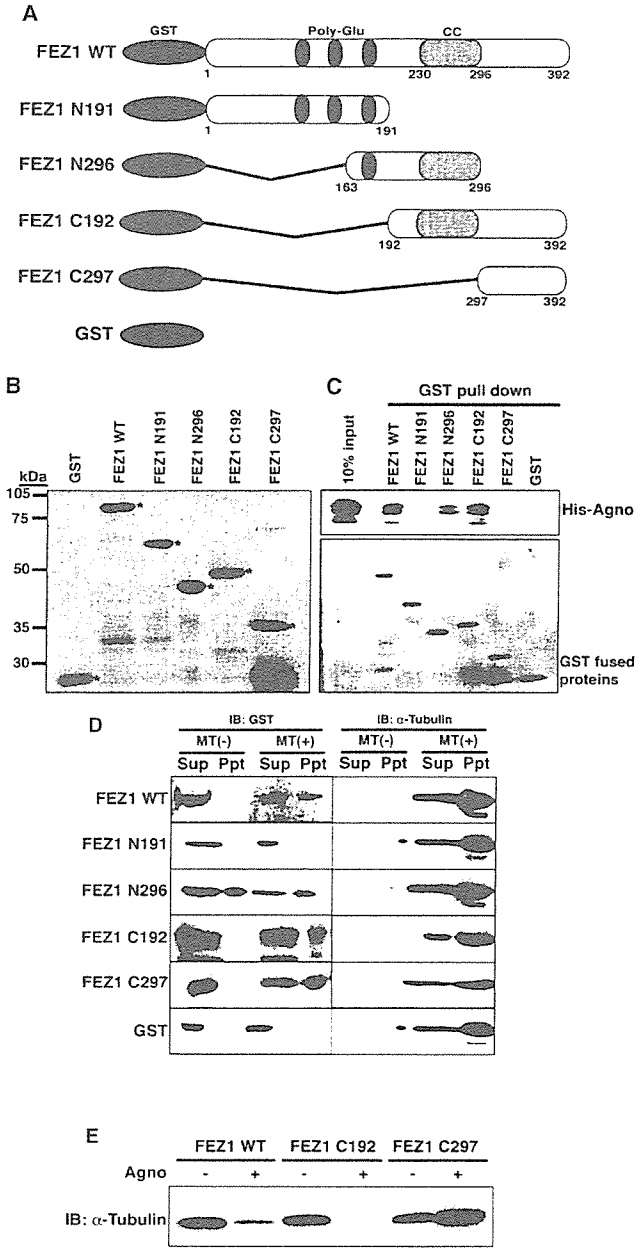

FIG. 4. **Delineation of the regions of FEZ1 that mediate interaction with microtubules and agnoprotein.** *A*, schematic representation of GST fusion constructs of wild-type (*WT*) FEZ1 and various FEZ1 deletion mutants. *B*, immunoblot analysis with antibodies to GST of the GST fusion proteins of FEZ1 deletion mutants purified from bacteria. *Asterisks* indicate the mature recombinant proteins. *C*, *in vitro* precipitation assay with the GST-FEZ1 deletion mutants and His-Agno. After incubation with His-Agno, the GST fusion proteins were precipitated with glutathione-Sepharose and bead-bound proteins were subjected to immunoblot analysis with antibodies to agnoprotein (*upper panel*) or to GST (*lower panel*). A portion of His-Agno corresponding to 10% of the input to the binding assay was also subjected directly to immunoblot analysis. *D*, microtubule cosedimentation assay performed with the GST fusion proteins of FEZ1 deletion mutants. The supernatant and precipitate fractions were subjected to immunoblot analysis with antibodies to GST. *E*, GST precipitation assay using GST-fused WT and mutant FEZ1 proteins and cell lysates from the agnoprotein-inducible cell line (293AG cells). After incubation with cell lysates, the GST fusion proteins were precipitated with glutathione-Sepharose, and bead-bound proteins were subjected to immunoblot analysis with antibodies to α-tubulin.

agnoprotein (Fig. 4*E*). These results suggested that the interaction of agnoprotein with FEZ1 at the CC domain is essential for disruption of interaction between microtubules and FEZ1 at the COOH-terminal region.

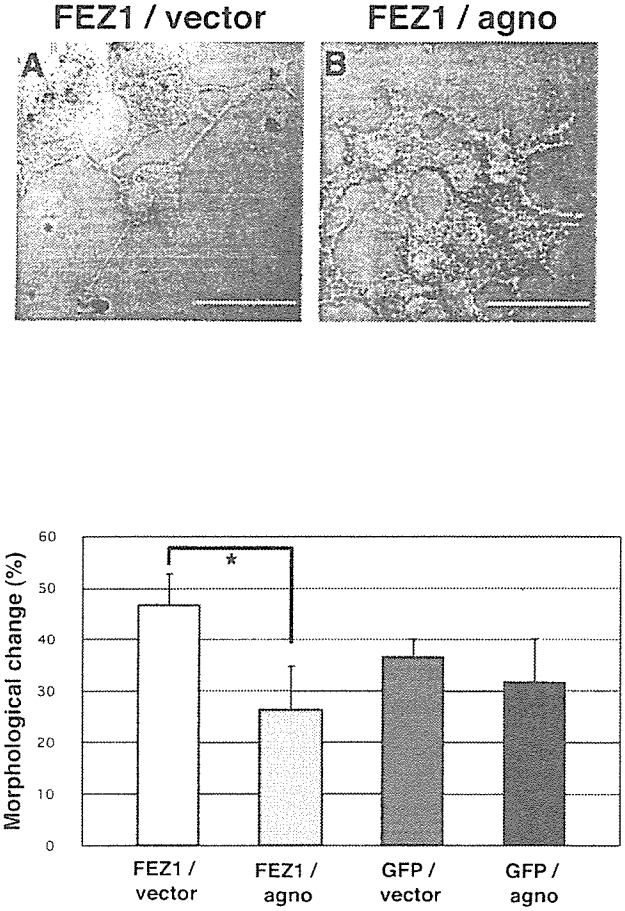

FIG. 5. **Agnoprotein-induced inhibition of the promotion of neurite outgrowth by FEZ1 in PC12 cells.** *A* and *B*, representative morphology of NGF-treated PC12 cells expressing FEZ1-GFP in the absence or presence of agnoprotein, respectively. The nuclei of transfected cells are colored *red* by DsRed. *Scale bars*, 50 μm. *C*, PC12 cells stably expressing GFP or FEZ1-GFP were transfected with the bicistronic expression vector pERedNLS-agno (*agno*) or pERedNLS (*vector*) and subsequently exposed to NGF. The cells were examined by fluorescence microscopy, and those that had been successfully transfected were identified by their DsRed-positive nuclei. The percentage of cells that underwent a morphological change, characterized in part by flattening of the cell body and extension of neurites with a length at least twice the diameter of the soma, was determined by evaluation of >300 cells with DsRed-positive nuclei. Data are means ± S.D. of values from three independent experiments. *, $p < 0.05$ for the indicated comparison (Student's *t* test).

Inhibition by Agnoprotein of the Promotion of Neurite Outgrowth by FEZ1 in PC12 Cells—FEZ1 has been implicated in axonal outgrowth and fasciculation (23) and promotes neurite extension in rat pheochromocytoma PC12 cells (37). We have now shown that FEZ1 associates with microtubules, and cytoskeletal filaments, including microtubules, are the final common target of various signaling cascades that influence development of the growth cone and neurite extension (39). To examine the possible effect of agnoprotein on the promotion of neurite outgrowth by FEZ1 in PC12 cells, which cease proliferation and begin to extend neurites in response to stimulation with NGF, we transfected PC12 cells that stably express FEZ1-GFP or GFP with pERedNLS-agno or the empty vector. Agnoprotein-expressing cells were thus labeled by expression of DsRed in the nucleus. Agnoprotein significantly inhibited neurite extension in NGF-treated cells that expressed FEZ1-GFP, but it had no effect on neurite outgrowth in NGF-treated cells expressing GFP (Fig. 5). These results suggested that agnoprotein inhibits the promotion of neurite outgrowth by FEZ1 in PC12 cells.

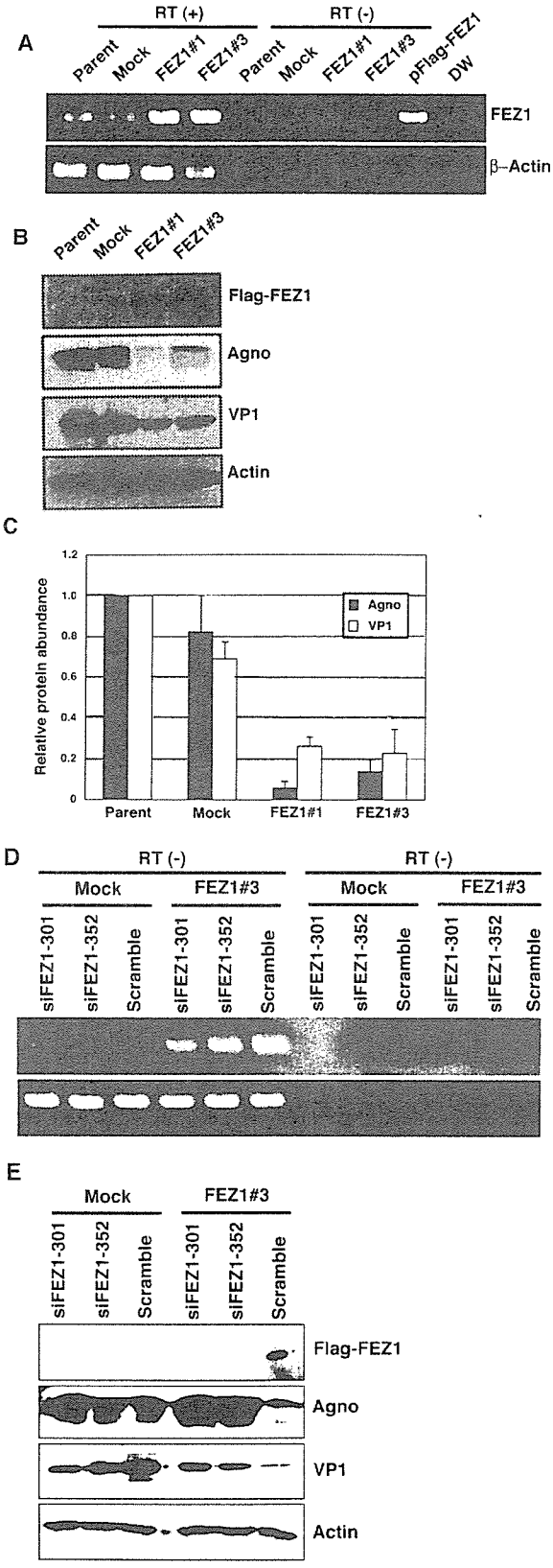

FIG. 6. **Suppression by FEZ1 of JCV protein expression in SVG-A cells inoculated with JCV.** *A*, RT-PCR analysis of FEZ1 mRNA (and β-actin mRNA) in SVG-A cells either stably expressing FLAG-FEZ1 (*FEZ1#1* and *FEZ1#3*) or stably transfected with the empty vector (*Mock*) as well as in parental SVG-A cells. The analysis was performed with or without RT. PCR controls were also performed with pFLAG-FEZ1 or distilled water (*DW*) as the template. *B*, immunoblot analysis of FEZ1#1, FEZ1#3, mock-transfected, and parental SVG-A cells lysed 7 days after inoculation with JCV (1000 hemagglutination units per 5×10^5 cells). The analysis was performed with antibodies to FLAG, to agnoprotein, to VP1, and to actin. *C*, the intensity of the immunoreactive bands corresponding to agnoprotein and VP1 in blots similar to that shown in *B* was quantified with an image analyzer and expressed relative to the values for parental SVG-A cells. Data are means ± S.D. of values from three independent experiments. *D*, RT-PCR analysis of FEZ1 mRNA (and β-actin mRNA) in FEZ1#3 cells or Mock cells transfected with siRNA against FEZ1 (*siFEZ1–301* and *siFEZ1–352*) or Scramble siRNA. *E*, immunoblot analysis of FEZ1#3 and mock-transfected SVG-A cells lysed 4 days after transfection with siRNA. These cells were inoculated with JCV (1000 hemagglutination units per 1×10^5 cells) on the preceding day of transfection. The analysis was performed with antibodies to FLAG, to agnoprotein, to VP1, and to actin.

Inhibition by FEZ1 of JCV Protein Expression in SVG-A Cells Inoculated with JCV—To examine the possible effects of FEZ1 on JCV infection in SVG-A cells, we established SVG-A cells that stably express FLAG-FEZ1. Given the lack of antibodies to FEZ1, we examined total (endogenous plus exogenous) FEZ1 expression by RT-PCR. The amount of FEZ1 mRNA in cells stably expressing FLAG-FEZ1 (FEZ1#1 and FEZ1#3 lines) was higher than that apparent in parental SVG-A cells or in cells stably transfected with the empty vector (Fig. 6*A*). The abundance of JCV agnoprotein and VP1 was markedly reduced in the cells expressing FLAG-FEZ1 compared with that apparent in control cells after inoculation with JCV (Fig. 6, *B* and *C*). To confirm if the effect for JCV infection in FLAG-FEZ1-expressing SVG-A cells depends on the expression of FEZ1, we used stealth siRNA (Invitrogen) to reduce the expression of FEZ1. At 24-h post inoculation of JCV, siRNAs (siFEZ1–301, siFEZ1–352, and Scramble) were transfected. The cells were harvested and analyzed by immunoblot at 96-h post transfection. The amount of FEZ1 mRNA in cells transfected with siFEZ1–301 or siFEZ1–352 siRNA was lower than that transfected with Scramble siRNAs (Fig. 6*D*). In the cells expressing FLAG-FEZ1, the abundance of JCV agnoprotein and VP1 was markedly increased in the cells transfected with siRNA to FEZ1 compared with Scramble siRNA. On the other hand, no difference was shown with cells transfected with siRNA to FEZ1 and Scramble in the cells stably transfected with the empty vector (Fig. 6*E*). FEZ1 thus suppressed the expression of JCV proteins in SVG-A cells. We also examined the transcriptional activity of JCV promoters in these various cell lines with a luciferase reporter assay but found no effect of FLAG-FEZ1 (data not shown).

Inhibition by FEZ1 of JCV Propagation in SVG-A Cells—Finally, we examined JCV-inoculated SVG-A cell lines by immunocytofluorescence analysis with antibodies to VP1. The number of VP1-positive cells did not differ significantly between either FEZ1#1 or FEZ1#3 cells and mock-transfected cells 3 days after inoculation (Fig. 7*A*). In contrast, the proportion of VP1-positive cells was significantly smaller for FEZ1#1 or FEZ1#3 cells than for mock-transfected cells 7 days after inoculation (Fig. 7), suggesting that FEZ1 suppressed the propagation of JCV in SVG-A cells. VP1 immunoreactivity was detected in the nucleus and cytoplasm of both parental and mock-transfected cells but was restricted to the nucleus in FEZ1#1 and FEZ1#3 cells 7 days after inoculation (Fig. 7*B*). These data suggested that FEZ1 suppressed the translocation of VP1 from the nucleus to the cytoplasm. We also analyzed the JCV inoculated cells by electron microscopy. This revealed that virion formation was intact in FEZ1-overexpressing cells (data not shown).

DISCUSSION

In the present study, we have identified FEZ1 as a binding partner of JCV agnoprotein. FEZ1 is a brain-specific protein and a mammalian homolog of *C. elegans* UNC-76 (23). Agno-

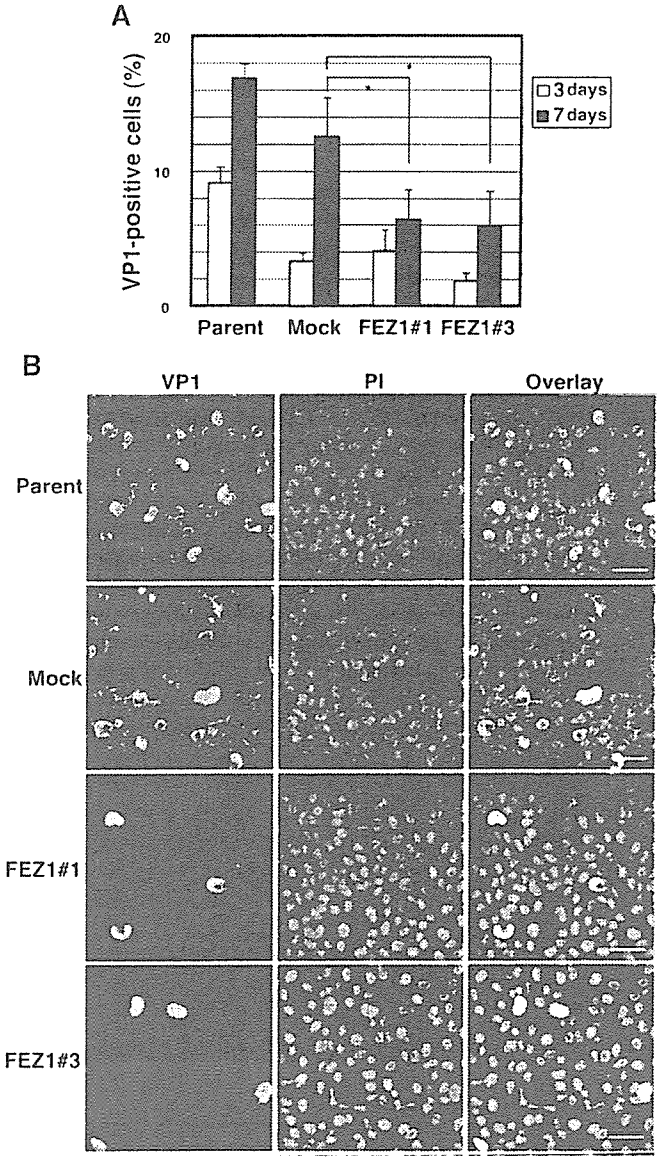

FIG. 7. **Suppression by FEZ1 of JCV propagation in SVG-A cells.** *A*, the proportion of VP1-positive cells among FEZ1#1, FEZ1#3, mock-transfected, and parental SVG-A cells determined by immunofluorescence analysis 3 and 7 days after inoculation with JCV as in Fig. 6. Data are means ± S.D. of values from three independent experiments. *, $p < 0.05$ for the indicated comparisons (Student's *t* test). *B*, immunostaining with antibodies to VP1 (*green*) of the indicated SVG-A cell lines at 7 days after inoculation with JCV. Cell nuclei were counterstained *red*. *Scale bars*, 50 μm.

protein interacted with FEZ1 in both yeast and mammalian cells and colocalized with both FEZ1 and microtubules in the perinuclear region of mammalian cells. We previously showed that agnoprotein colocalizes with microtubules (38), and we here confirmed the binding of agnoprotein to microtubules with a microtubule cosedimentation assay. Microtubules are a major component of the cytoskeleton in growing axons, and, together with their associated molecules, they play an important role in axon outgrowth (39). We have now shown that FEZ1, which promotes axon outgrowth in PC12 cells (37), also binds to microtubules in the microtubule cosedimentation assay and that the interaction between FEZ1 and microtubules is disrupted by agnoprotein. Regions of FEZ1 that mediate interaction with microtubules and agnoprotein are not the same, and the binding of agnoprotein with the CC domain of FEZ1 plays a pivotal role in disruption of interaction between microtubules and FEZ1. These results suggest that the interaction of agnoprotein with FEZ1 might lead to some conformational changes in the COOH-terminal region of FEZ1, resulting in lost of its ability to combine with microtubules.

The promotion of neurite outgrowth by FEZ1 in PC12 cells was also inhibited by agnoprotein. These results suggest that FEZ1 might promote neurite extension through interaction with microtubules and that this interaction is sensitive to agnoprotein. Overexpression of FEZ1 in human glial cells inhibited the production of JCV agnoprotein and VP1 without affecting transcription from JCV promoters. Although the number of JCV-infected cells did not differ between SVG-A cells stably expressing FEZ1 and control cells at 3 days after inoculation with JCV, the proportion of VP1-positive cells was markedly reduced by FEZ1 overexpression at 7 days. These results suggest that overexpression of FEZ1 influenced the late phase of JCV infection but did not affect the early phase, including the attachment of JCV to cells, its entry into the cytoplasm, and transcription of the JCV genome. Whereas VP1 was present in both the nucleus and cytoplasm of control cells at 7 days after inoculation with JCV, it was restricted to the nucleus of cells overexpressing FEZ1. Given that the antibodies to VP1 used for these experiments recognize both VP1 monomers and mature virus particles, our results suggest that both VP1 monomers and mature JCV virions were restricted to the nucleus of cells stably expressing FEZ1. A mutational analysis of SV40 agnoprotein similarly showed that this protein plays an important role in the release of progeny virions from infected cells and in viral propagation (14–16). The transport of progeny virions of SV40 from the nucleus to the cell surface depends on intracytoplasmic vesicular transport (40). We have detected JCV virions both in the cytoplasm of infected cells and in the surrounding extracellular space in the apparent absence of disruption of the cell membrane both in progressive multifocal leukoencephalopathy lesions and in cell cultures (19). These observations indicate that JCV virions might be released from host cells by a specific mechanism and that FEZ1 might inhibit JCV release from infected human cells.

UNC-76 of *Drosophila*, which is a homolog of FEZ1, binds specifically to the tail domain of kinesin heavy chain in the yeast two-hybrid system and copurification assays. Furthermore, immunostaining and genetic analyses have demonstrated that UNC-76 function is required for axonal transport in the *Drosophila* nervous system (41). Interestingly, we observed that FEZ1 interacted with KIF3A that is a member of KIF3 family by immunoprecipitation assay (data not shown). These observations thus suggest that UNC-76 and FEZ1 play an essential role in kinesin-mediated transport pathways. Kinesin is a plus end-directed microtubule motor that facilitates the movement of vesicles, messenger ribonucleoproteins, and organelles. It was first identified in squid axoplasm as a protein that facilitates ATP-dependent vesicle movement along microtubules (42, 43). Subsequent molecular, genetic, and biochemical studies have shown that kinesin is required for intracellular transport in eukaryotes in many cellular contexts (44–46).

The requirement for kinesin-based transport is especially prominent in polarized cells such as neurons. The polarity complex comprised of PAR3, PAR6, and atypical protein kinase C (PKC) contributes to polarity determination in many tissues and cells (47, 48). FEZ1 was also identified in a yeast two-hybrid assay for proteins that bind the regulatory domain of the rat atypical PKC isoform PKCζ (37). Whereas nonphosphorylated FEZ1 is associated with both cytosolic and membrane fractions of COS-7 cells, its phosphorylation by PKCζ induces the redistribution of membrane-bound FEZ1 to the cytosol. In addition, the phosphorylation of FEZ1 by PKCζ stimulates

neurite outgrowth in PC12 cells. These observations suggest that FEZ1, like UNC-76, might associate with kinesin and is essential for PKCζ-dependent neuronal differentiation.

FEZ1 also interacts in neural cells with the protein Disrupted-In-Schizophrenia 1, which was identified as the product of a gene disrupted by a (1;11)(q42.1;q14.3) chromosomal translocation that segregates with schizophrenia in a Scottish family. Furthermore, interaction of Disrupted-In-Schizophrenia 1 and FEZ1 appears to take place on or near the actin cytoskeleton and is up-regulated during neurite outgrowth (49).

The actin and tubulin cytoskeletons are a final common target of many signaling cascades that influence neuronal development (39), and cytoskeletal dynamics and polarized axonal transport appear to be closely related (50, 51). Our observation that FEZ1 associates with microtubules, combined with its possible interaction with kinesin and the previous finding that it promotes neurite outgrowth, suggest that FEZ1 may play a key role downstream of atypical PKC and the polarity complex in the regulation of vesicle trafficking that contributes to neurite extension.

Although the release of mature progeny virions of SV40 and JCV assembled in the nucleus has been thought to occur through disintegration or rupture of infected cells, these viruses do not encode an enzyme that is able to cause cell lysis. In addition, progeny virions of SV40 have been shown to be transported from the nucleus to the cell surface in a manner dependent on vesicular transport (40). The tegument protein US11 of herpes simplex virus, another DNA virus, interacts with conventional kinesin heavy chain, and this interaction has been thought to be important for anterograde transport of nonenveloped nucleocapsids in axons (52). The transport and release of large numbers of virus particles are undesirable for host cells. It is thus possible that FEZ1 serves a potentially protective function in JCV-infected cells by inhibiting the release of progeny virions. Interestingly, expression of FEZ1 in JCV-permissible cells such as SVG-A cells or IMR-32 cells is much less than nonpermissible neuronal cells (53) such as SH-SY5Y cells (data not shown). This suggests that expression levels of FEZ1 might be a factor that determines JCV tissue specificity. Conversely, the viral agnoprotein may inhibit the physiological function of FEZ1 by inducing its dissociation from microtubules, thereby promoting the effective transmission of progeny viruses.

Acknowledgments—We thank M. Sato and S. Nakagaki for expert technical assistance and Dr. W. W. Hall, Dr. C. Henmi, Y. Makino, and T. Aketagawa for their valuable suggestions.

REFERENCES

1. Frisque, R. J., Bream, G. L., and Cannella, M. T. (1984) *J. Virol.* **51,** 458–469
2. Safak, M., Gallia, G. L., Ansari, S. A., and Khalili, K. (1999) *J. Virol.* **73,** 10146–10157
3. Safak, M., Gallia, G. L., and Khalili, K. (1999) *Mol. Cell. Biol.* **19,** 2712–2723
4. Gallia, G. L., Safak, M., and Khalili, K. (1998) *J. Biol. Chem.* **273,** 32662–32669
5. Major, E. O., Amemiya, K., Tornatore, C. S., Houff, S. A., and Berger, J. R. (1992) *Clin. Microbiol. Rev.* **5,** 49–73
6. Safak, M., Barrucco, R., Darbinyan, A., Okada, Y., Nagashima, K., and Khalili, K. (2001) *J. Virol.* **75,** 1476–1486
7. Cohen, E. A., Subbramanian, R. A., and Gottlinger, H. G. (1996) *Curr. Top. Microbiol. Immunol.* **214,** 219–235
8. Cullen, B. R. (1998) *Cell* **93,** 685–692
9. Michaud, G., Zachary, A., Rao, V. B., and Black, L. W. (1989) *J. Mol. Biol.* **209,** 667–681
10. Terwilliger, E. F., Cohen, E. A., Lu, Y. C., Sodroski, J. G., and Haseltine, W. A. (1989) *Proc. Natl. Acad. Sci. U. S. A.* **86,** 5163–5167
11. Strebel, K., Klimkait, T., Maldarelli, F., and Martin, M. A. (1989) *J. Virol.* **63,** 3784–3791
12. Harris, M. (1999) *Curr. Biol.* **9,** R459–R461
13. Hou-Jong, M. H., Larsen, S. H., and Roman, A. (1987) *J. Virol.* **61,** 937–939
14. Resnick, J., and Shenk, T. (1986) *J. Virol.* **60,** 1098–1106
15. Carswell, S., Resnick, J., and Alwine, J. C. (1986) *J. Virol.* **60,** 415–422
16. Carswell, S., and Alwine, J. C. (1986) *J. Virol.* **60,** 1055–1061
17. Ressetar, H. G., Walker, D. L., Webster, H. D., Braun, D. G., and Stoner, G. L. (1990) *Lab. Invest.* **62,** 287–296
18. Shishido-Hara, Y., Hara, Y., Larson, T., Yasui, K., Nagashima, K., and Stoner, G. L. (2000) *J. Virol.* **74,** 1840–1853
19. Okada, Y., Sawa, H., Endo, S., Orba, Y., Umemura, T., Nishihara, H., Stan, A. C., Tanaka, S., Takahashi, H., and Nagashima, K. (2002) *Acta Neuropathol. (Berl.)* **104,** 130–136
20. Nomura, S., Khoury, G., and Jay, G. (1983) *J. Virol.* **45,** 428–433
21. Okada, Y., Endo, S., Takahashi, H., Sawa, H., Umemura, T., and Nagashima, K. (2001) *J. Neurovirol.* **7,** 302–306
22. Orba, Y., Sawa, H., Iwata, H., Tanaka, S., and Nagashima, K. (2004) *J. Virol.* **78,** 7270–7273
23. Bloom, L., and Horvitz, H. R. (1997) *Proc. Natl. Acad. Sci. U. S. A.* **94,** 3414–3419
24. Tokui, M., Takei, I., Tashiro, F., Shimada, A., Kasuga, A., Ishii, M., Ishii, T., Takatsu, K., Saruta, T., and Miyazaki, J. (1997) *Biochem. Biophys. Res. Commun.* **233,** 527–531
25. Ashok, A., and Atwood, W. J. (2003) *J. Virol.* **77,** 1347–1356
26. Nukuzuma, S., Yogo, Y., Guo, J., Nukuzuma, C., Itoh, S., Shinohara, T., and Nagashima, K. (1995) *J. Med. Virol.* **47,** 370–377
27. Fujita, T., Ikuta, J., Hamada, J., Okajima, T., Tatematsu, K., Tanizawa, K., and Kuroda, S. (2004) *Biochem. Biophys. Res. Commun.* **313,** 738–744
28. Suzuki, S., Sawa, H., Komagome, R., Orba, Y., Yamada, M., Okada, Y., Ishida, Y., Nishihara, H., Tanaka, S., and Nagashima, K. (2001) *Virology* **286,** 100–112
29. Komagome, R., Sawa, H., Suzuki, T., Suzuki, Y., Tanaka, S., Atwood, W. J., and Nagashima, K. (2002) *J. Virol.* **76,** 12992–13000
30. Okada, Y., Sawa, H., Tanaka, S., Takada, A., Suzuki, S., Hasegawa, H., Umemura, T., Fujisawa, J., Tanaka, Y., Hall, W. W., and Nagashima, K. (2000) *J. Biol. Chem.* **275,** 17016–17023
31. Qu, Q., Sawa, H., Suzuki, T., Semba, S., Henmi, C., Okada, Y., Tsuda, M., Tanaka, S., Atwood, W. J., and Nagashima, K. (2004) *J. Biol. Chem.* **279,** 27735–27742
32. Pierre, P., Scheel, J., Rickard, J. E., and Kreis, T. E. (1992) *Cell* **70,** 887–900
33. Takakuwa, H., Goshima, F., Koshizuka, T., Murata, T., Daikoku, T., and Nishiyama, Y. (2001) *Genes Cells* **6,** 955–966
34. Fukata, Y., Itoh, T. J., Kimura, T., Menager, C., Nishimura, T., Shiromizu, T., Watanabe, H., Inagaki, N., Iwamatsu, A., Hotani, H., and Kaibuchi, K. (2002) *Nature Cell Biol.* **4,** 583–591
35. Hergovich, A., Lisztwan, J., Barry, R., Ballschmieter, P., and Krek, W. (2003) *Nature Cell Biol.* **5,** 64–70
36. Higuchi, O., Amano, T., Yang, N., and Mizuno, K. (1997) *Oncogene* **14,** 1819–1825
37. Kuroda, S., Nakagawa, N., Tokunaga, C., Tatematsu, K., and Tanizawa, K. (1999) *J. Cell Biol.* **144,** 403–411
38. Endo, S., Okada, Y., Orba, Y., Nishihara, H., Tanaka, S., Nagashima, K., and Sawa, H. (2003) *J. Neurovirol.* **9,** Suppl. 1, 10–14
39. Dent, E. W., and Gertler, F. B. (2003) *Neuron* **40,** 209–227
40. Clayson, E. T., Brando, L. V., and Compans, R. W. (1989) *J. Virol.* **63,** 2278–2288
41. Gindhart, J. G., Chen, J., Faulkner, M., Gandhi, R., Doerner, K., Wisniewski, T., and Nandlestadt, A. (2003) *Mol. Biol. Cell* **14,** 3356–3365
42. Brady, S. T. (1985) *Nature* **317,** 73–75
43. Vale, R. D., Reese, T. S., and Sheetz, M. P. (1985) *Cell* **42,** 39–50
44. Martin, M., Iyadurai, S. J., Gassman, A., Gindhart, J. G., Jr., Hays, T. S., and Saxton, W. M. (1999) *Mol. Biol. Cell* **10,** 3717–3728
45. Goldstein, L. S. (2001) *Proc. Natl. Acad. Sci. U. S. A.* **98,** 6999–7003
46. Stebbings, H. (2001) *Int. Rev. Cytol.* **211,** 1–31
47. Etienne-Manneville, S., and Hall, A. (2003) *Curr. Opin. Cell Biol.* **15,** 67–72
48. Fukata, M., Nakagawa, M., and Kaibuchi, K. (2003) *Curr. Opin. Cell Biol.* **15,** 590–597
49. Miyoshi, K., Honda, A., Baba, K., Taniguchi, M., Oono, K., Fujita, T., Kuroda, S., Katayama, T., and Tohyama, M. (2003) *Mol. Psychiatry* **8,** 685–694
50. Nakata, T., and Hirokawa, N. (2003) *J. Cell Biol.* **162,** 1045–1055
51. Setou, M., Hayasaka, T., and Yao, I. (2004) *J. Neurobiol.* **58,** 201–206
52. Diefenbach, R. J., Miranda-Saksena, M., Diefenbach, E., Holland, D. J., Boadle, R. A., Armati, P. J., and Cunningham, A. L. (2002) *J. Virol.* **76,** 3282–3291
53. Shinohara, T., Nagashima, K., and Major, E. O. (1997) *Virology* **228,** 269–277

JOURNAL OF VIROLOGY, Mar. 2005, p. 2910–2919 Vol. 79, No. 5
0022-538X/05/$08.00+0 doi:10.1128/JVI.79.5.2910–2919.2005

Synthetic Double-Stranded RNA Poly(I:C) Combined with Mucosal Vaccine Protects against Influenza Virus Infection

Takeshi Ichinohe,[1,2] Izumi Watanabe,[1,2] Satoshi Ito,[1,2] Hideki Fujii,[3] Masami Moriyama,[4] Shin-ichi Tamura,[5] Hidehiro Takahashi,[1] Hirofumi Sawa,[6] Joe Chiba,[2] Takeshi Kurata,[1] Tetsutaro Sata,[1] and Hideki Hasegawa[1]*

Department of Pathology, National Institute of Infectious Diseases, Musashimurayama-shi,[1] Department of Immunology, National Institute of Infectious Diseases, Toyama, Shinjuku-ku,[3] and Department of Microbiology and Immunology, School of Medicine, Keio University, Shinano-machi, Shinjyuku-ku,[4] Tokyo, Department of Biological Science and Technology, Tokyo University of Science, Yamazaki, Noda, Chiba,[2] Laboratory of Prevention of Viral Diseases, Research Institute for Microbial Diseases, Osaka University, Yamadaoka, Suita, Osaka,[5] and Laboratory of Molecular & Cellular Pathology, 21st Century COE, Program for Zoonosis Control, Hokkaido University School of Medicine, and CREST, JST, Kita-ku, Sapporo,[6] Japan

Received 13 July 2004/Accepted 21 October 2004

The mucosal adjuvant effect of synthetic double-stranded RNA polyriboinosinic polyribocytidylic acid [poly(I:C)] against influenza virus was examined under intranasal coadministration with inactivated hemagglutinin (HA) vaccine in BALB/c mice and was shown to have a protective effect against both nasal-restricted infection and lethal lung infection. Intranasal administration of vaccine from PR8 (H1N1) with poly(I:C) induced a high anti-HA immunoglobulin A (IgA) response in the nasal wash and IgG antibody response in the serum, while vaccination without poly(I:C) induced little response. Intracerebral injection confirmed the safety of poly(I:C). In addition, we demonstrated that administration of poly(I:C) with either A/Beijing (H1N1) or A/Yamagata (H1N1) vaccine conferred complete protection against PR8 challenge in this mouse nasal infection model, suggesting that poly(I:C) possessed cross-protection ability against variant viruses. To investigate the mechanism of the protective effect of poly(I:C), mRNA levels of Toll-like receptors and cytokines were examined in the nasal-associated lymphoid tissue after vaccination or virus challenge. Intranasal administration of HA vaccine with poly(I:C) up-regulated expression of Toll-like receptor 3 and alpha/beta interferons as well as Th1- and Th2-related cytokines. We propose that poly(I:C) is a new effective intranasal adjuvant for influenza virus vaccine.

When developing a vaccine, both prophylactic effectiveness and safety should be considered. It has been reported that the respiratory tract (RT) mucosal immune system is usually the first immunological barrier against influenza virus infection (16, 17, 36) and a primary site of influenza virus infection. The influenza virus causes annual epidemics of influenza by altering the antigenic properties of its surface hemagglutinin (HA), which is involved in binding of sialic acids to the surface of susceptible cells (23). Inactivated vaccines against the influenza virus have been administered parenterally to induce serum anti-HA immunoglobulin G (IgG) antibodies (Abs) that are highly protective against homologous virus infection but are less effective against heterologous virus infection (19, 23). In contrast, a number of studies have shown that the mucosal immunity acquired by natural infection, which is mainly due to the secreted form of IgA (s-IgA) in the RT, is more effective and cross-protective against virus infections than systemic immunity induced by parenteral vaccines in humans (4, 5, 11, 18, 23) and mice (15, 36). In this regard, induction of s-IgA at the RT has a great advantage in protecting against unpredictable epidemics of influenza.

* Corresponding author. Mailing address: Department of Pathology, National Institute of Infectious Diseases, 4-7-1 Gakuen, Musashimurayama-shi, Tokyo 208-0011, Japan. Phone: 81-42-561-0771. Fax: 81-42-561-6572. E-mail: hasegawa@nih.go.jp.

We have demonstrated that intranasal immunization with an inactivated vaccine together with cholera toxin B subunits (CTB) containing a trace amount of holotoxin (CTB*) induces not only s-IgA with strong cross-protection against infection by variant viruses belonging to the same subtype in the upper RT but also serum IgG with weak cross-protection against variant virus infection in the lower RT in mice (26, 30–32). These findings were consistent with those of previous reports (13, 20, 22). Although CTB* is an effective adjuvant to produce s-IgA, it has some side effects, such as nasal discharge in humans. Several attempts to reduce the side effects have been carried out by introduction of mutations in CTB (8) or using physiological adjuvants, such as complement component C3d (37). Therefore, there is a need for an adjuvant that is both as effective as CTB* and safe for human use for the clinical application of intranasal influenza virus vaccine.

Double-stranded RNA (dsRNA) acts as a molecular mimic associated with viral infection, because most viruses produce dsRNA during their replication (10). It has also been shown that mammalian Toll-like receptor 3 (TLR3) recognizes dsRNA and activates the NF-κB (1) pathway, resulting in activation of alpha/beta interferon (IFN-α/β), which enhances the primary antibody response against subcutaneous immunization of soluble materials (14). The adjuvant activity of IFN-α/β seems to play an important role in bridging the gap between innate and adaptive immunity (14).

In the present study, we demonstrated that the mucosal adjuvant activity of intranasal administration of synthetic dsRNA polyriboinosinic polyribocytidylic acid [poly(I:C)] with inactivated influenza virus HA vaccine induced cross-protective immune responses against homologous and heterologous variant influenza virus infection.

MATERIALS AND METHODS

HA vaccines and influenza viruses. HA vaccines (split-product virus vaccines) were prepared from influenza viruses, including A/Puerto Rico/3/334 (A/PR8; H1N1), A/Yamagata/120/86 (A/Yamagata; H1N1), A/Beijing/262/95 (A/Beijing; H1N1), A/Guizhou/54/89 (A/Guizhou; H3N2), B/Ibaraki/2/85 (B/Ibaraki), B/Aichi/5/88 (B/Aichi), and B/Yamagata/16/88 (B/Yamagata) strains according to the method of Davenport et al. (6) at the Kitasato Institute (Saitama, Japan). These viruses were grown in allantoic cavities from 10- to 11-day-old fertile chicken eggs, purified, and disintegrated with ethyl ether. The vaccine contained all proteins from virus particles. However, the major component of the vaccine was HA molecules (about 30% of total protein). The PR/8 virus used for the challenge experiments was adapted to mice by subculturing 148 times in ferrets, 596 times in mice, and 73 times in 10-day-old fertile chicken eggs.

Preparation of adjuvants. Cholera toxin B subunits containing a trace amount of holotoxin were prepared by adding 0.1% CT (holotoxin) to CTB obtained from Sigma (St. Louis, Mo.). Synthetic double-stranded RNA poly(I:C) was kindly provided by Toray Industries, Inc. (Kamakura, Kanagawa, Japan). Heat-denatured double-stranded RNA poly(I:C), which was boiled at 95°C for 5 min and cooled immediately on ice, was used as a negative control.

Immunization with vaccine and virus challenge. Female BALB/c mice (Japan SLC Inc., Hamamatsu, Japan), age 6 to 8 weeks at the time of immunization, were used in all experiments. All animal experiments were carried out in accordance with the Guides for Animal Experiments Performed at NIID and approved by the Animal Care and Use Committee of the National Institute of Infectious Diseases.

Five mice for each experimental group were anesthetized with diethyl ether and immunized primarily by dropping 5 μl of phosphate-buffered saline (PBS) containing 1 μg of HA vaccine with 0.1 to 10 μg of poly(I:C) into each nostril. Four weeks later, they were reimmunized in the same manner with or without the same adjuvant.

According to a modification of the procedure of Yetter and coworkers (27, 29, 38), each mouse was anesthetized and infected by intranasal administration of 1 μl of PBS containing virus suspension with 1,000 PFU of mouse-adapted PR8 virus into each nostril. As 1 μl of the virus suspension remained in the local nasal area and could not enter the lung tissue, the initial viral infection was limited to the nasal area. To examine cross-reactivity of poly(I:C) treatment against variant influenza virus subtypes, the mice were immunized intranasally with various vaccines (1 μg) together with poly(I:C) (3 μg) and boosted with each vaccine alone 4 weeks later. Two weeks after the second immunization, the immunized mice were challenged by upper RT infection with the A/PR8 virus, and 3 days later nasal wash and serum specimens were collected for virus and Ab titration.

Measurement of the virus titer and anti-PR8 HA antibodies. Serum, nasal wash fluid, and bronchoalveolar wash fluid were collected for measurement of virus titer and antibodies against PR8 HA from mice that were sacrificed under anesthesia with chloroform. The levels of IgA and IgG Abs against HA molecules purified from the A/PR8 viruses were determined by enzyme-linked immunosorbent assay (ELISA) as described previously (29). Briefly, ELISA was conducted sequentially from the solid phase (EIA plate; Costar, Cambridge, Mass.) with a ladder of reagents consisting of the following: first, HA molecules purified from the A/PR8 virus according to the procedure of Phelan et al. (21); second, nasal wash fluid, bronchoalveolar wash fluid, or serum; third, either goat anti-mouse IgA Ab (α-chain specific; Amersham) or goat anti-mouse IgG antibody (γ-chain-specific anti-IgG antibody; Amersham), or anti-mouse IgG1 and IgG2a (BD Pharmingen, San Diego, Calif.) conjugated with biotin; fourth, streptavidin conjugated with alkaline phosphatase (Life Technologies, Rockville, Md.); and fifth, *p*-nitrophenylphosphate. The chromogen produced was measured by determining the absorbance at 405 nm with an ELISA reader. A twofold serial dilution of either purified HA-specific IgA (320 ng/ml) or HA-specific monoclonal IgG (160 ng/ml) was used as a standard as described previously (2). The binding kinetics of the standard HA-specific monoclonal IgG were comparable to purified HA-specific IgG from immunized mice. In the IgG subtype assay, HA-specific monoclonal IgG1 and normal mouse serum were used as controls. The HA-specific monoclonal antibody was recognized exclusively by anti-mouse IgG1 antibody but not by anti-mouse IgG2a antibody. No HA-specific IgG1 or IgG2a was detected in normal mouse serum. To examine whether poly(I:C) is effective for protection against influenza virus-induced lethal pneumonia, mice were challenged with a lethal dose (1,000 PFU in 20 μl) of PR8 virus at 2 weeks after the second immunization. The survival rate of the mice was estimated at 2 weeks after the viral challenge. The viral titer of the lung wash fluid was examined 3 days after the challenge (see Fig. 2). The antibody concentrations of unknown specimens were determined from the standard regression curve constructed for each assay with a programmed SJeia Autoreader (model er-8000; Sanko Jun-yaku, Tokyo, Japan).

Virus neutralization by antisera was determined as previously described (3). Briefly, virus was mixed with inactivated antisera from naive or vaccinated mice at 37°C for 1 h, and the mixture was added to Madin-Darby canine kidney (MDCK) cells in a total volume of 200 μl. The neutralizing capacity of antisera was measured by comparing the reduction in the number of infected cells per sample to sera from age-matched naive mice. Inhibition of virus was assessed by the additional reduction in infectivity beyond the background of naive-mouse antisera. Inhibition was measured by 50% inhibition of virus infection (beyond nonspecific inhibition). Samples were run in duplicate assays on the same day and averaged, and data are presented as the average per group.

The virus titer was measured as follows: aliquots of 200 μl of serial 10-fold dilutions of the nasal wash fluid were inoculated into MDCK cells in six-well plates. After a 1-h incubation, each well was overlaid with 2 ml of agar medium according to the method of Tobita and coworkers (34, 35). The number of plaques in each well was counted at 2 days after inoculation. All of the experiments were repeated independently at least three times. The data are presented as means ± standard deviations (SD).

RNA isolation, cDNA synthesis, and real-time PCR. The expression of TLR3 and TLR4 in nasal-associated lymphoid tissues (NALTs) in vaccinated or influenza virus-infected mice was examined. Mice were inoculated with influenza virus or intranasally administered influenza virus HA vaccine with or without poly(I:C). The NALTs were collected sequentially up to 72 h after administration. The mRNA levels of TLR3 and TLR4 in the NALTs were measured by real-time quantitative PCR after reverse transcription. Total RNA was extracted from the NALTs in mice by using an SV-Total RNA isolation kit (Promega, Madison, Wis.) and cDNA was synthesized using Omniscript reverse transcriptase (QIAGEN, Valencia, Calif.) according to the manufacturer's instructions.

Real-time quantitative PCR was performed using the ABI PRISM 7900 sequence detection system (Applied Biosystems, Foster City, Calif.) with a QuantiTect Probe PCR kit (QIAGEN), TaqMan probes (Applied Biosystems), and primers (Sigma Genosys, Ishikari, Japan) listed in Table 1 designed with Primer Express (Applied Biosystems). The system uses two dye layers to detect the presence of target and control sequences. The FAM (6-carboxyfluorescein) dye layer yields results for quantification of the cytokine target mRNA. The cytokine and TLR targets examined were IFN-α, IFN-β, IFN-γ, interleukin-4 (IL-4), IL-6, IL-12 p40, TLR-3, and TLR-4. PCR was carried out in a volume of 20 μl: initial denaturation at 50°C for 2 min and 95°C for 15 min was followed by 45 cycles of 94°C for 15 s and 60°C for 1 min. For each sample, PCR was performed in duplicate. cDNA levels were determined using the standard curve of cycle thresholds. All data obtained were normalized to the β-actin cDNA level.

Effects of intracerebral injection of poly(I:C). Seven-week-old BALB/c female mice were injected intracerebrally with poly(I:C) or CTB* at various doses [0.25, 2.5, or 25 μg for poly(I:C) and 2.5, 10, or 25 μg for CTB*] in 25 μl of PBS, and their mortality and body weights were monitored for 7 days. PBS was used as a negative control.

Antigen-specific T-cell response. Antigen-specific T-cell responses were measured as previously described (24). Spleens were harvested from mice 1 week after the boost vaccination. After the preparation of a single cell suspension, T cells were purified by depletion of $CD11b^+$ (Mac-1), $CD45R^+$ (B220), $DX5^+$, and $Ter\text{-}119^+$ cells by using a magnetic cell sorting system (MACS; Miltenyi Biotec, Bergisch, Germany). To prepare antigen-presenting cells, normal BALB/c mouse splenocytes were depleted of $CD90\ (Thy1.2)^+$ cells by MACS and irradiated at 2,000 cGy.

Purified T cells taken from the spleen (10^5 cells/well) were cultured with irradiated antigen-presenting cells (5×10^5 cells/well) in the presence or absence of PR8 vaccine (0.1, 1, or 10 μg/ml). Four days after the cultivation, the level of cytokine concentration in the culture supernatant was measured by ELISA using a mouse IFN-γ immunoassay kit (Biosource International, Camarillo, Calif.) according to the manufacturer's instruction. T-cell proliferation was monitored by the incorporation of [^{3}H]thymidine (18.5 kBq/well; ICN Biomedicals, Costa Mesa, Calif.) added 8 h prior to cell harvest. The cells were harvested on a 96-well microplate bonded with a GF/B filter (Packard Instruments, Meriden, Conn.). Incorporated radioactivity was counted by a microplate scintillation counter (Packard Instruments).